



**UNIVERSITI PUTRA MALAYSIA**

***SYNTHESIS AND DIELECTRIC PROPERTIES OF  
Bi<sub>3.36</sub>Mg<sub>1.92-x</sub>A<sub>x</sub>Nb<sub>2.72</sub>O<sub>13.76</sub> (A = Ca, Sr AND Ba) PYROCHLORE  
SYSTEMS***

**NURUL AIDAYU BINTI MAT DASIN**

**FS 2018 17**



**SYNTHESIS AND DIELECTRIC PROPERTIES OF  
 $\text{Bi}_{3.36}\text{Mg}_{1.92-x}\text{A}_x\text{Nb}_{2.72}\text{O}_{13.76}$  (A = Ca, Sr AND Ba) PYROCHLORE SYSTEMS**

By

**NURUL AIDAYU BINTI MAT DASIN**

**Thesis Submitted to the School of Graduate Studies, Universiti Putra Malaysia, in  
Fulfilment of the Requirements for the Degree of Master of Science**

**November 2017**

## **COPYRIGHT**

All material contained within the thesis, including without limitation text, logos, icons, photographs and all other artwork, is copyright material of Universiti Putra Malaysia unless otherwise stated. Use may be made of any material contained within the thesis for non-commercial purposes from the copyright holder. Commercial use of material may only be made with the express, prior, written permission of Universiti Putra Malaysia.

Copyright © Universiti Putra Malaysia



Abstract of thesis presented to the Senate of Universiti Putra Malaysia in fulfillment of the requirement for the degree of Master of Science

**SYNTHESIS AND DIELECTRIC PROPERTIES OF  
Bi<sub>3.36</sub>Mg<sub>1.92-x</sub>A<sub>x</sub>Nb<sub>2.72</sub>O<sub>13.76</sub> (A = Ca, Sr AND Ba) PYROCHLORE SYSTEMS**

By

**NURUL AIDAYU BINTI MAT DASIN**

**November 2017**

**Chairman: Tan Kar Ban, PhD**  
**Faculty: Science**

Bismuth magnesium niobate (BMN) pyrochlores are one of the potential dielectrics owing to their excellent dielectric properties, e.g. high relative permittivity,  $\epsilon' > 160$ , low dielectric loss,  $\tan \delta$  in the order of  $\sim 10^{-4}$  and compositional tunable temperature coefficient of capacitance, TCC. In this work, alkaline earth metals namely, Ca, Sr and Ba were successfully introduced into BMN pyrochlores through solid-state reaction. These substitutional solid solutions were prepared with the proposed chemical formula,  $(\text{Bi}_{3.36}\text{Mg}_{0.64-x}\text{A}_x)(\text{Mg}_{1.28}\text{Nb}_{2.72})\text{O}_{13.76}$ , in which the formation mechanism requires a one-to-one replacement of  $\text{Mg}^{2+}$  by  $\text{A}^{2+}$  ( $\text{A}^{2+} = \text{Ca, Sr and Ba}$ ) at the eight-coordinated A site. The solid solution limits of  $(\text{Bi}_{3.36}\text{Mg}_{0.64-x}\text{A}_x)(\text{Mg}_{1.28}\text{Nb}_{2.72})\text{O}_{13.76}$  are found to be  $0 \leq x \leq 0.7$ ,  $0 \leq x \leq 0.5$  and  $0 \leq x \leq 0.2$  in the Ca-, Sr- and Ba-series, respectively. Ca-doped BMN pyrochlores have a relatively extensive solid solution limit due to the closely similar ionic radii between  $\text{Ca}^{2+}$  and  $\text{Bi}^{3+}$  with their values of 1.12 Å and 1.13 Å, respectively. These materials adopted a cubic symmetry, space group Fd3m (No. 277),  $Z = 4$ , with their refined lattice parameters,  $a = b = c$ , decrease linearly from 10.5968(16) Å to 10.5332(14) Å, 10.5671(17) Å and 10.5879(3) Å, respectively. On the other hand, all BMCN, BMSN and BMBN pyrochlores are found to be thermally stable as thermal event is absent within the studied temperature range  $\sim 30$ –1000 °C. Whilst, the irregular shaped grains of surface morphologies of these samples showing a broad distribution of mean grain size with increasing of dopant concentration. Six IR-active phonon modes are observed in these chemically doped pyrochlores, which are due to the vibration and bending of metal-oxygen bond in the range  $1000 \text{ cm}^{-1}$ – $200 \text{ cm}^{-1}$ .

All the doped BMN pyrochlores appeared to be highly insulating with their conductivities in the order of  $\sim 10^{-6}$ – $10^{-5} \text{ Scm}^{-1}$  at  $\sim 600$  °C. These materials exhibited moderate high  $\epsilon'$ , low  $\tan \delta$  in the order of  $10^{-3}$ – $10^{-1}$  at  $\sim 30$  °C and negative TCC values,  $\sim 319$ – $933 \text{ ppm}/^\circ\text{C}$  in the temperature range  $\sim 30$ – $300$  °C. The recorded  $\epsilon'$  values of Ca-, Sr- and Ba-series are in the range 69–171, 90–186 and 147–183, respectively at  $\sim 30$  °C and 1 MHz. The Arrhenius conductivity plots of these doped BMN pyrochlores showed linear and reversible characteristics in a heat-cool cycle. The activation energies of BMCN, BMSN and BMBN pyrochlores are found in the range

1.17–1.47 eV, 1.20–1.49 eV and 1.18–1.30 eV, respectively. The high activation energies,  $E_a > 1.0$  eV are required for the electrical conduction, which is probably of a hopping electronic type.

In attempts to investigate the electrical properties of pyrochlores in electrolyte, further studies have been performed by using pyrochlore thin films coated on indium tin oxide (ITO) glasses using cyclic voltametry (CV), galvanostatic charge-discharge (CD) and electrochemical impedance spectroscopy (EIS), respectively. Higher specific capacitance is recorded for 1-layer sample compared to 3- and 5-layer sample coated on ITO glasses in 1.0 M KCl electrolyte. The specific capacitance of 1-layer sample is found to decrease with increasing dopant concentration in respective Ca- Sr- and Ba-series. On the other hand, the cyclic voltammogram curves of all the samples showed rectangular in shape without any pseudocapacitance effect, which is a common capacitive behaviour of electrochemical supercapacitors.

Abstrak tesis yang dikemukakan kepada Senat Universiti Putra Malaysia sebagai memenuhi keperluan untuk ijazah Sarjana Sains

**SINTESIS DAN SIFAT DIELEKTRIK PIROKLOR DALAM SISTEM**  
 **$\text{Bi}_{3.36}\text{Mg}_{1.92-x}\text{A}_x\text{Nb}_{2.72}\text{O}_{13.76}$  (A = Ca, Sr DAN Ba)**

Oleh

**NURUL AIDAYU BINTI MAT DASIN**

**November 2017**

**Pengerusi: Tan Kar Ban, PhD**  
**Fakulti: Sains**

Piroklor yang mengandungi bismut magnesium niobat (BMN) adalah salah satu daripada dielektrik yang berpotensi disebabkan oleh ciri-ciri dielektrik yang menarik. Di antara ciri-ciri tersebut adalah, pemalar dielektrik yang tinggi,  $\epsilon' > 160$ , kehilangan dielektrik yang rendah,  $\tan \delta$  dalam lingkungan  $\sim 10^{-4}$  dan pekali suhu kapasitan yang boleh ubah mengikut komposisi, TCC. Dalam kajian ini, logam alkali bumi, iaitu, Ca, Sr dan Ba telah berjaya diganti ke dalam piroklor BMN dengan kaedah keadaan pepejal. Larutan pepejal penggantian ini disediakan dengan menggunakan formula kimia yang dicadangkan seperti berikut,  $(\text{Bi}_{3.36}\text{Mg}_{0.64-x}\text{A}_x)(\text{Mg}_{1.28}\text{Nb}_{2.72})\text{O}_{13.76}$ , di mana mekanisme pembentukan sistem ini memerlukan penggantian setiap  $\text{Mg}^{2+}$  dengan  $\text{A}^{2+}$  ( $\text{A}^{2+} = \text{Ca}, \text{Sr}$  dan  $\text{Ba}$ ) di tapak A yang berkoordinasi lapan. Julat larutan pepejal dalam sistem  $(\text{Bi}_{3.36}\text{Mg}_{0.64-x}\text{A}_x)(\text{Mg}_{1.28}\text{Nb}_{2.72})\text{O}_{13.76}$  adalah  $0 \leq x \leq 0.7$ ,  $0 \leq x \leq 0.5$  dan  $0 \leq x \leq 0.2$  untuk siri Ca, Sr dan Ba. Piroklor BMN yang didop dengan Ca mempunyai julat larutan pepejal yang lebih ekstensif jika dibandingkan dengan siri  $\text{Sr}^{2+}$  dan  $\text{Ba}^{2+}$ . Ini disebabkan oleh persamaan saiz jejari ion antara  $\text{Ca}^{2+}$  dan  $\text{Bi}^{3+}$  yang hampir sama iaitu 1.12 Å dan 1.13 Å. Bahan-bahan ini mengahablur dengan simetri kubik, kumpulan ruang  $\text{Fd}3\text{m}$  (No. 277),  $Z = 4$ , dengan parameter kekisi terproses,  $a = b = c$  yang menunjukkan penurunan secara linear dalam semua siri. Nilai penurunan tersebut adalah daripada 10.5968(16) Å kepada 10.5332(14) Å (siri Ca), 10.5671(17) Å (siri Sr) dan 10.5879(3) Å (siri Ba). Selain daripada itu, semua piroklor BMCN, BMSN dan BMBN didapati stabil kerana tidak menunjukkan sebarang peristiwa terma dalam julat suhu yang dikaji iaitu di antara  $\sim 30$ – $1000$  °C. Manakala, morfologi permukaan untuk semua sampel-sampel dalam siri Ca, Sr dan Ba telah menunjukkan butiran yang tak sekata dan taburan purata saiz butiran yang luas serta saiz yang meningkat dengan kepekatan bahan pendop. Sebanyak enam mod fonon telah dikenalpasti sebagai IR yang aktif bagi semua siri piroklor BMN yang telah didopkan. Keseluruhan mod fonon disebabkan oleh ikatan antara logam dengan oksigen yang bergetar dan membengkok dalam julat suhu  $1000 \text{ cm}^{-1}$ – $200 \text{ cm}^{-1}$ .

Semua siri piroklor BMN yang didopkan mempunyai kerintangan yang tinggi dengan kekonduksian di antara  $\sim 10^{-6}$ – $10^{-5} \text{ Scm}^{-1}$  pada suhu  $\sim 600$  °C. Bahan-bahan ini didapati mempunyai sifat pemalar dielektrik,  $\epsilon'$  yang sederhana tinggi,  $\tan \delta$  yang rendah dalam

jumlah  $10^{-3}$ – $10^{-1}$  pada suhu  $\sim 30$  °C dan nilai TCC yang negatif yaitu  $\sim 319$  hingga  $\sim 933$  ppm/°C dalam julat suhu  $\sim 30$ – $300$  °C. Nilai  $\epsilon'$  yang direkodkan oleh siri Ca, Sr dan Ba adalah dalam lingkungan 69–171, 90–186 dan 147–183 pada suhu  $\sim 30$  °C dan 1 MHz. Lakaran kekonduksian Arrhenius bagi piroklor BMN yang didopkan telah menunjukkan ciri-ciri linear dan berbalik dalam kitaran pemanasan dan penyejukan. Tenaga pengaktifan untuk piroklor BMCN, BMSN dan BMBN adalah dalam julat 1.17–1.47 eV, 1.20–1.49 eV dan 1.18–1.30 eV. Tenaga pengaktifan yang tinggi,  $E_a > 1.0$  eV biasanya diperlukan untuk pengaliran elektrik yang disebabkan oleh mekanisme elektron lompatan.

Dalam usaha penyiasatan mengenai sifat elektrik piroklor dalam elektrolit, kajian lanjutan telah dilakukan dengan menggunakan filem nipis piroklor pada kaca oksida indium timah (ITO). Kesemua kajian ini telah dijalankan dengan menggunakan larutan elektrolit KCl yang mempunyai kepekatan 1.0 M secara kitaran voltametri (CV), cas dan nyahcas (CD) dan spektroskopi impedans elektrokimia (EIS). Kapasitan spesifik yang tinggi telah direkodkan oleh sampel yang disalutkan dengan satu lapisan pada kaca ITO jika dibandingkan dengan tiga atau lima lapisan yang menunjukkan nilai kapasitan spesifik yang lebih rendah. Nilai kapasitan spesifik yang disalutkan dengan satu lapisan sampel merosot dengan peningkatan kepekatan bahan pendop untuk kesemua siri Ca, Sr dan Ba. Selain daripada itu, semua sampel menunjukkan kitaran lengkung voltammogram yang sama iaitu berbentuk segiempat tepat tanpa sebarang kesan pseudokapasitan dan ini menunjukkan sifat kapasitif yang biasa dalam superkapasitor elektrokimia.

## ACKNOWLEDGEMENTS

First and foremost, I would like to convey my utmost gratitude to my project supervisor, Assoc. Prof. Dr. Tan Kar Ban who has guided me with his patience and supports throughout the entire course of this project. He has made a great effort by giving his invaluable advice, constructive suggestion and discussion. His constant encouragement and belief have inspired me to strike harder in this project. I would like to extend my sincere appreciation to my co-supervisors, Dr. Khaw Chien Chieh and Prof. Dr. Zulkarnain Zainal for their guidance and insightful suggestion.

I would like to thank the staff of the Department of Chemistry especially Madam Zaidina Mohd Daud (XRD), Madam Rusnani Amirudin (FTIR), Madam Nor Azlina Shari (DTA, TGA) and Madam Nurhidayu Jamaludin (ICP-OES) for their technical assistance and guidance in my data collection. My appreciation also dedicated to all the staff from the Electron Microscopy Unit, UPM and the Department of Physics, UPM.

A special thanks to my seniors, Dr. Chon Mun Ping and Dr. Tan Phei Yi who have rendered their helps at the beginning of my research journey. Not to be forgotten is Dr. Chang Sook Keng who has helped and guided me in electrochemical impedance spectroscopy (EIS) measurements. In my lab, I have been blessed to have a friendly and cheerful group of comrades and friends. My sincere thanks extended to Ms. Syazmimi, Ms. Syafiqah, Ms. Kartika, Mr. Chuah You Jian, Ms. Chan Siew Ling and Ms. Hidayah for their kindness and supports. Also, a heartfelt appreciation to my beloved friend, Ms. Woon Yen Ling who is always there for me and trust what I could achieve thus far. Last but not least, my deepest affection and gratitude to my beloved family who are always there to listen my problems and give me moral supports, prayers and advices, which ultimately motivate me to move forward.



I certify that a Thesis Examination Committee has met on 15 November 2017 to conduct the final examination of Nurul Aidayu bt Mat Dasin on her thesis entitled "Synthesis and Dielectric Properties of  $\text{Bi}_{3.36}\text{Mg}_{1.92-x}\text{A}_x\text{Nb}_{2.72}\text{O}_{13.76}$  (A = Ca, Sr and Ba) Pyrochlore Systems" in accordance with the Universities and University Colleges Act 1971 and the Constitution of the Universiti Putra Malaysia [P.U.(A) 106] 15 March 1998. The Committee recommends that the student be awarded the Master of Science.

Members of the Thesis Examination Committee were as follows:

**Jaafar bin Abdullah, PhD**

Senior Lecturer  
Faculty of Science  
Universiti Putra Malaysia  
(Chairman)

**Tan Yen Ping, PhD**

Senior Lecturer  
Faculty of Science  
Universiti Putra Malaysia  
(Internal Examiner)

**Oi Boon Hong, PhD**

Associate Professor  
University of Malaya  
Malaysia  
(External Examiner)



---

**NOR AINI AB. SHUKOR, PhD**

Professor and Deputy Dean  
School of Graduate Studies  
Universiti Putra Malaysia

Date: 28 December 2017

This thesis was submitted to the Senate of Universiti Putra Malaysia and has been accepted as fulfillment of the requirement for the degree of Master of Science. The members of the Supervisory Committee were as follows:

**Tan Kar Ban, PhD**

Associate Professor  
Faculty of Science  
Universiti Putra Malaysia  
(Chairman)

**Zulkarnain bin Zainal, PhD**

Professor  
Faculty of Science  
Universiti Putra Malaysia  
(Member)

**Khaw Chwin Chieh, PhD**

Senior Lecturer  
Universiti Tunku Abdul Rahman  
Malaysia  
(Member)

---

**ROBIAH BINTI YUNUS, PhD**

Professor and Dean  
School of Graduate Studies  
Universiti Putra Malaysia

Date:

## Declaration by graduate student

I hereby confirm that:

- this thesis is my original work;
- quotations, illustrations and citations have been duly referenced;
- this thesis has not been submitted previously or concurrently for any other degree at any other institutions;
- intellectual property from the thesis and copyright of thesis are fully-owned by Universiti Putra Malaysia, as according to the Universiti Putra Malaysia (Research) Rules 2012;
- written permission must be obtained from supervisor and the office of Deputy Vice-Chancellor (Research and Innovation) before thesis is published (in the form of written, printed or in electronic form) including books, journals, modules, proceedings, popular writings, seminar papers, manuscripts, posters, reports, lecture notes, learning modules or any other materials as stated in the Universiti Putra Malaysia (Research) Rules 2012;
- there is no plagiarism or data falsification/ fabrication in the thesis, and scholarly integrity is upheld as according to the Universiti Putra Malaysia (Graduate Studies) Rules 2003 (Revision 2012-2013) and the Universiti Putra Malaysia (Research) Rules 2012. The thesis has undergone plagiarism detection software.

Signature: \_\_\_\_\_ Date: \_\_\_\_\_

Name and Matric No.: Nurul Aidayu Binti Mat Dasin (GS 41233)

## Declaration by Members of Supervisory Committee

This is to confirm that:

- the research conducted and the writing of this thesis was under our supervision;
- supervision responsibilities as stated in the Universiti Putra Malaysia (Graduate Studies) Rules 2003 (Revision 2012-2013) are adhered to.

Signature : \_\_\_\_\_  
Name of Chairman of Supervisory Committee : Assoc. Prof. Dr. Tan Kar Ban

Signature : \_\_\_\_\_  
Name of Member of Supervisory Committee : Prof. Dr. Zulkarnain Zainal

Signature : \_\_\_\_\_  
Name of Member of Supervisory Committee : Dr. Khaw Chwin Chieh

## TABLE OF CONTENTS

	<b>Page</b>
<b>ABSTRACT</b>	i
<b>ABSTRAK</b>	iii
<b>ACKNOWLEDGEMENTS</b>	v
<b>APPROVAL</b>	vi
<b>DECLARATION</b>	viii
<b>LIST OF TABLES</b>	xii
<b>LIST OF FIGURES</b>	xiv
<b>LIST OF ABBREVIATIONS</b>	xxi
<b>CHAPTER</b>	
<b>1. INTRODUCTION</b>	1
1.1 The Fundamental of Ceramic	1
1.1.1 Electroceramics	1
1.2 Dielectric Materials	6
1.2.1 Dielectric Constant	6
1.2.1.1 Polarisation	7
1.2.2 Dielectric Loss	11
1.2.3 Temperature Coefficient of Capacitance (TCC)	12
1.3 Applications of Dielectric Ceramics	13
1.3.1 Low Temperature Co-fired Ceramics (LTCC)	13
1.3.2 Multilayer Ceramic Capacitors (MLCC)	13
1.4 Problem Statements	14
1.5 Objectives	14
<b>2. LITERATURE REVIEW</b>	15
2.1 Overview of Pyrochlores	15
2.2 Bismuth-based Pyrochlores and Related Materials	20
2.2.1 Bismuth Zinc Niobate (BZN) Ternary System	22
2.2.2 Bismuth Magnesium Tantalate (BMT) and Bismuth Magnesium Niobate (BMN) Pyrochlore Systems	26
2.2.3 Chemically Doped BMT and BMN Pyrochlore Systems	29
<b>3. METHODOLOGY</b>	31
3.1 Conventional Solid-state Reaction	31
3.2 Sample Preparation	31
3.2.1 Synthesis of Alkaline Earth Metals Doped Pyrochlores	31
3.2.2 Pelletised Samples	32
3.2.3 Pyrochlore Thin Films on ITO (Indium Tin Oxide) Glass	32
3.3 Characterisation and Analyses	33
3.3.1 Powder X-ray Diffraction Spectroscopy (XRD)	34
3.3.2 Thermal Analyses (TGA and DTA)	35
3.3.3 Scanning Electron Microscopy (SEM)	36
3.3.4 Fourier Transform Infrared Spectroscopy (FT-IR)	37
3.3.5 Elemental Analyses	37
3.3.5.1 Inductively Coupled Plasma Optical Emission Spectroscopy (ICP-OES)	37

3.3.5.2	X-ray Fluorescence Spectroscopy(XRF)	38
3.3.6	Electrical Properties	39
3.3.6.1	AC Impedance Spectroscopy	39
3.3.6.2	Cole-cole Plot	39
3.3.6.3	Electric Modulus Spectroscopy	41
3.3.6.4	Experimental Procedure	42
3.3.7	Electrochemical Impedance Spectroscopy (EIS)	43
3.3.7.1	Electrochemical Measurement	48
<b>4.</b>	<b>RESULTS AND DISCUSSION</b>	<b>50</b>
4.1	$\text{Bi}_{1.36}\text{Mg}_{1.92-x}\text{Ca}_x\text{Nb}_{2.72}\text{O}_{13.76}$ (BMCN) Pyrochlore System	51
4.1.1	Solid Solution Formation, Elemental and Thermal Analyses	51
4.1.2	Structural and Surface Morphology Studies	58
4.1.2.1	Fourier Transform Infrared Spectroscopy (FT-IR)	58
4.1.2.2	Scanning Electron Microscopy (SEM)	60
4.1.3	Electrical Properties	65
4.1.4	Conclusion	72
4.2	$\text{Bi}_{1.36}\text{Mg}_{1.92-x}\text{Sr}_x\text{Nb}_{2.72}\text{O}_{13.76}$ (BMSN) Pyrochlore System	72
4.2.1	Solid Solution Formation, Elemental and Thermal Analyses	72
4.2.2	Structural and Surface Morphology Studies	78
4.2.2.1	Fourier Transform Infrared Spectroscopy (FT-IR)	78
4.2.2.2	Scanning Electron Microscopy (SEM)	80
4.2.3	Electrical Properties	85
4.2.4	Conclusion	92
4.3	$\text{Bi}_{1.36}\text{Mg}_{1.92-x}\text{Ba}_x\text{Nb}_{2.72}\text{O}_{14.36}$ (BMBN) Pyrochlore System	92
4.3.1	Solid Solution Formation, Elemental and Thermal Analyses	92
4.3.2	Structural and Surface Morphology Studies	98
4.3.2.1	Fourier Transform Infrared Spectroscopy (FT-IR)	98
4.3.2.2	Scanning Electron Microscopy (SEM)	100
4.3.3	Electrical Properties	104
4.3.4	Conclusion	111
4.4	Electrochemical Measurement	112
4.4.1	BMCN, BMSN and BMBN Pyrochlores Prepared by Dip-coating Method in 1.0 M KCl Electrolyte	112
4.4.2	Cyclic Voltametry (CV) Analyses	112
4.4.3	Galvanostatic Charge-discharge (CD) Analyses	116
4.4.4	Electrochemical Impedance Spectroscopy (EIS) Analyses	130
4.4.5	Conclusion	133
<b>5.</b>	<b>CONCLUSION</b>	<b>134</b>
5.1	Conclusions	134
5.2	Recommendations for Future Research	135
	<b>REFERENCES</b>	<b>136</b>
	<b>APPENDICES</b>	<b>149</b>
	<b>BIODATA OF STUDENT</b>	<b>158</b>
	<b>LIST OF PUBLICATIONS</b>	<b>159</b>

## LIST OF TABLES

Table		Page
1.1	List of some ceramic conductor materials used in different applications (Moulson and Herbert, 2003).	2
1.2	List of few conductive ceramic materials used as solid electrolytes in sensor to sense different elements and compounds (Moulson and Herbert, 2003).	2
1.3	Different types of magnetism with the susceptibility value of some materials (Moulson and Herbert, 2003).	3
1.4	Typical materials of low and high temperature co-fired ceramic systems (Christou, 2006).	13
2.1	The phonon modes in the infrared of BZN pyrochlore at 300 K and 50 K (Chen <i>et al.</i> , 2005).	25
2.2	Comparison of the dielectric constant in bismuth-based pyrochlore at the different frequencies.	29
3.1	Wavelengths used in ICP-OES analysis.	38
3.2	Capacitance values and possible region.	41
4.1	Indexed pattern of $\text{Bi}_{3.36}\text{Mg}_{1.92}\text{Nb}_{2.72}\text{O}_{13.76}$ (BMN) cubic pyrochlore.	51
4.2	Elemental concentrations of BMCN solid solution using ICP-OES.	55
4.3	Elemental concentrations of BMCN solid solution using XRF.	56
4.4	Phonon mode in IR spectrum of $(\text{Bi}_{3.36}\text{Mg}_{0.64-x}\text{Ca}_x)(\text{Mg}_{1.28}\text{Nb}_{2.72})\text{O}_{13.76}$ ( $0 \leq x \leq 0.7$ ) pyrochlores at 300 K.	60
4.5	Crystallite sizes and strains of $(\text{Bi}_{3.36}\text{Mg}_{0.64-x}\text{Ca}_x)(\text{Mg}_{1.28}\text{Nb}_{2.72})\text{O}_{13.76}$ ( $0 \leq x \leq 0.7$ ) pyrochlore.	65
4.6	Summary of $\epsilon'$ , $\tan \delta$ , TCC, $E_a$ and $r_A/r_B$ of $(\text{Bi}_{3.36}\text{Mg}_{0.64-x}\text{Ca}_x)(\text{Mg}_{1.28}\text{Nb}_{2.72})\text{O}_{13.76}$ ( $0 \leq x \leq 0.7$ ) pyrochlores.	71
4.7	Elemental concentrations of $(\text{Bi}_{3.36}\text{Mg}_{0.64-x}\text{Sr}_x)(\text{Mg}_{1.28}\text{Nb}_{2.72})\text{O}_{13.76}$ solid solution using ICP-OES.	77
4.8	Elemental concentrations of $(\text{Bi}_{3.36}\text{Mg}_{0.64-x}\text{Sr}_x)(\text{Mg}_{1.28}\text{Nb}_{2.72})\text{O}_{13.76}$ solid solution using XRF.	78
4.9	Phonon mode in IR spectrum of Sr doped BMN pyrochlores at 300 K.	80

4.10	Calculated grain sizes, crystallite sizes and strains of $(\text{Bi}_{3.36}\text{Mg}_{0.64-x}\text{Sr}_x)(\text{Mg}_{1.28}\text{Nb}_{2.72})\text{O}_{13.76}$ ( $0 \leq x \leq 0.5$ ) pyrochlore electroceramics.	84
4.11	Summary of dielectric constant ( $\epsilon'$ ), dielectric loss ( $\tan \delta$ ), temperature coefficient of capacitance ( $\text{ppm}/^\circ\text{C}$ ) and activation energy ( $E_a$ ) of $(\text{Bi}_{3.36}\text{Mg}_{0.64-x}\text{Sr}_x)(\text{Mg}_{1.28}\text{Nb}_{2.72})\text{O}_{13.76}$ ( $0 \leq x \leq 0.5$ ) pyrochlore.	91
4.12	Elemental concentrations of $(\text{Bi}_{3.36}\text{Mg}_{0.64-x}\text{Ba}_x)(\text{Mg}_{1.28}\text{Nb}_{2.72})\text{O}_{14.36}$ solid solution using ICP-OES.	96
4.13	Elemental concentrations of $(\text{Bi}_{3.36}\text{Mg}_{0.64-x}\text{Ba}_x)(\text{Mg}_{1.28}\text{Nb}_{2.72})\text{O}_{14.36}$ solid solution using XRF.	96
4.14	IR phonon modes of BMBN solid solution at 300 K.	99
4.15	Calculated grain sizes, crystallite sizes and strains of BMBN pyrochlores.	104
4.16	Summary of dielectric constants ( $\epsilon'$ ), dielectric loss ( $\tan \delta$ ), temperature coefficient of capacitance ( $\text{ppm}/^\circ\text{C}$ ) and activation energy ( $E_a$ ) of BMBN pyrochlores.	105
4.17	The calculated specific capacitances of 1-, 3- and 5-layer at various current densities of BMCN ( $0 \leq x \leq 0.7$ ) systems.	124
4.18	The calculated specific capacitances of 1-, 3- and 5-layer at various current densities of BMSN ( $0 \leq x \leq 0.5$ ) systems.	125
4.19	The calculated specific capacitances of 1-, 3- and 5-layer at various current densities of BMBN ( $0 \leq x \leq 0.2$ ) systems.	126
4.20	Cell electrolyte resistance ( $R_s$ ) and Faradaic charge-transfer resistance ( $R_{ct}$ ) obtained from impedance analyses.	132



## LIST OF FIGURES

Figure		Page
1.1	Description of a diamagnetic material in the absence of a magnetic field and when a field is applied (Goldman, 2006).	4
1.2	Schematic diagram of spins in a paramagnetic solid (Riedel and Chen, 2014).	4
1.3	Schematic diagram of spins in a ferromagnetic material and ferromagnetic hysteresis loops (Riedel and Chen, 2014).	5
1.4	Frequency dependence of polarisation processes and peak power losses (Kim and Tadokoro, 2007).	8
1.5	The total negative charge $-Ze$ is distributed homogenously throughout the sphere of R (a) while the nucleus and electron cloud are displaced in opposite direction (b) (Maheshwari, 2006).	9
1.6	Ionic polarisation measures shift of ions relative to each other and electronic polarisation measures shift of electron cloud relative to nucleus within the atom (Maheshwari, 2006).	10
1.7	Orientation polarisation produced in the case of a polar molecule of an electric field (Maheshwari, 2006).	11
1.8	Space charge polarisation (Maheshwari, 2006).	11
2.1	The two independent and interpenetrating 3D networks of cubic pyrochlores crystal structure resulting $A_2B_2O_6O'/A_2B_2O_7$ (Vanderah <i>et al.</i> , 2005).	15
2.2a	Pyrochlore structure showing the two distinct cation sites, which were A cation of eight-coordinated (6+2 fold) and B cation of six-coordinated (octahedron) (Subramanian <i>et al.</i> , 1983).	16
2.2b	Pyrochlore structure derived from fluorite lattice, cubic Fd3m showing at Wyckoff positions and crystallographically type lattice (Subramanian <i>et al.</i> , 1983).	16
2.3	The pyrochlore structure based on corner shared $BO_6$ octahedral (Subramanian <i>et al.</i> , 1983).	17
2.4	The pyrochlore structure defined in two interpenetrating networks of $BO_6$ octahedral and $A_2O'$ chains (Subramanian <i>et al.</i> , 1983).	18
2.5	Possible substitutions at A and B sites of oxide pyrochlores $A_2^{3+}B_2^{4+}O_7$ type (Subramanian <i>et al.</i> , 1983).	19

2.6	Possible substitutions at A and B sites of oxide pyrochlores $A_2^{2+}B_2^{5+}O_7$ type (Subramanian <i>et al.</i> , 1983).	19
3.1	Summary for sample preparation using conventional solid state method.	32
3.2	Summary for sample preparation using ITO.	33
3.3	Summary of sample preparation and characterisation.	34
3.4	Schematic diagram on X-rays diffraction works (Garrison, 2003).	34
3.5	Complex plane plot with the equivalent circuit (Abram <i>et al.</i> , 2001).	40
3.6	Combined $Z''$ and $M''$ against logarithmic frequency (Sinclair <i>et al.</i> , 2000).	42
3.7	Sinusoidal voltage and current signal during an impedance measurement (Illig, 2014).	44
3.8	The schematic diagram of a simple electrochemical cell (Bard <i>et al.</i> , 2012).	45
3.9	The impedance plot of an electrochemical system (Conway, 1999; Beguin and Frackowiak, 2010).	46
3.10	Typical CV curve (Conway, 1999; Beguin and Frackowiak, 2010).	47
3.11	$Q$ discharge vs. Ewe plot, which is used to calculate p slope from equation below (Conway, 1999; Beguin and Frackowiak, 2010).	47
3.12	The typical curve of galvanostatic charge-discharge process. (1) The cell behavior during charging, (2) The cell behavior during discharging, (3) The initial process and (4) This section is responsible for the negative resistive ohmic lost associated with the resistance of the cell (Conway, 1999; Beguin and Frackowiak, 2010).	48
4.1a	XRD patterns of $(Bi_{3.36}Mg_{0.64-x}Ca_x)(Mg_{1.28}Nb_{2.72})O_{13.76}$ ( $0 \leq x \leq 0.7$ ) solid solution.	52
4.1b	XRD patterns of BMCN at $x = 0.8$ .	52
4.2	Variation of lattice parameters in BMCN pyrochlores.	53
4.3	TGA thermograms of $(Bi_{3.36}Mg_{0.64-x}Ca_x)(Mg_{1.28}Nb_{2.72})O_{13.76}$ ( $0 \leq x \leq 0.7$ ) solid solution.	57
4.4	DTA thermograms of $(Bi_{3.36}Mg_{0.64-x}Ca_x)(Mg_{1.28}Nb_{2.72})O_{13.76}$ ( $0 \leq x$	57

	$\leq 0.7$ ) solid solution.	
4.5	IR spectra of $(\text{Bi}_{3.36}\text{Mg}_{0.64-x}\text{Ca}_x)(\text{Mg}_{1.28}\text{Nb}_{2.72})\text{O}_{13.76}$ ( $0 \leq x \leq 0.7$ ) solid solution.	59
4.6	SEM micrographs of BMCN samples recorded at magnification of 3 k.	61
4.7	Grain size distribution of BMCN pyrochlores.	62
4.8	Comparison of crystallite sizes between Scherrer and Williamson-Hall methods and the internal strain for each composition of BMCN.	63
4.9	Williamson-hall plot with five intense x-ray diffraction peaks of $(\text{Bi}_{3.36}\text{Mg}_{0.64-x}\text{Ca}_x)(\text{Mg}_{1.28}\text{Nb}_{2.72})\text{O}_{13.76}$ ( $0 \leq x \leq 0.7$ ) pyrochlores.	64
4.10	Complex impedance plot of $\text{Bi}_{3.36}\text{Mg}_{1.22}\text{Ca}_{0.7}\text{Nb}_{2.72}\text{O}_{13.76}$ at 650 °C.	66
4.11	Combine spectroscopic plots of $\text{Bi}_{3.36}\text{Mg}_{1.22}\text{Ca}_{0.7}\text{Nb}_{2.72}\text{O}_{13.76}$ .	66
4.12	Imaginary part of impedance plotted as a function of frequency at different temperatures for composition, $\text{Bi}_{3.36}\text{Mg}_{1.22}\text{Ca}_{0.7}\text{Nb}_{2.72}\text{O}_{13.76}$ .	67
4.13	Arrhenius conductivity plots of $(\text{Bi}_{3.36}\text{Mg}_{0.64-x}\text{Ca}_x)(\text{Mg}_{1.28}\text{Nb}_{2.72})\text{O}_{13.76}$ ( $0 \leq x \leq 0.7$ ) cubic pyrochlores.	68
4.14	Temperature dependence of dielectric constant of $(\text{Bi}_{3.36}\text{Mg}_{0.64-x}\text{Ca}_x)(\text{Mg}_{1.28}\text{Nb}_{2.72})\text{O}_{13.76}$ ( $0 \leq x \leq 0.7$ ) cubic pyrochlores.	70
4.15	Dielectric loss as a function of temperature for $(\text{Bi}_{3.36}\text{Mg}_{0.64-x}\text{Ca}_x)(\text{Mg}_{1.28}\text{Nb}_{2.72})\text{O}_{13.76}$ ( $0 \leq x \leq 0.7$ ) cubic pyrochlores.	71
4.16a	XRD patterns of $(\text{Bi}_{3.36}\text{Mg}_{0.64-x}\text{Sr}_x)(\text{Mg}_{1.28}\text{Nb}_{2.72})\text{O}_{13.76}$ ( $0 \leq x \leq 0.5$ ) solid solution.	73
4.16b	XRD patterns of BMSN at $x = 0.6$ .	73
4.17a	Variation of lattice parameters in $(\text{Bi}_{3.36}\text{Mg}_{0.64-x}\text{Sr}_x)(\text{Mg}_{1.28}\text{Nb}_{2.72})\text{O}_{13.76}$ ( $0 \leq x \leq 0.5$ ) pyrochlores.	74
4.17b	Constant shift of (222) diffraction plane towards higher angle.	75
4.18	TGA thermograms of $(\text{Bi}_{3.36}\text{Mg}_{0.64-x}\text{Sr}_x)(\text{Mg}_{1.28}\text{Nb}_{2.72})\text{O}_{13.76}$ ( $0 \leq x \leq 0.5$ ) solid solution.	76
4.19	DTA thermograms of $(\text{Bi}_{3.36}\text{Mg}_{0.64-x}\text{Sr}_x)(\text{Mg}_{1.28}\text{Nb}_{2.72})\text{O}_{13.76}$ ( $0 \leq x \leq 0.5$ ) solid solution.	76

4.20	IR spectra of $(\text{Bi}_{3.36}\text{Mg}_{0.64-x}\text{Sr}_x)(\text{Mg}_{1.28}\text{Nb}_{2.72})\text{O}_{13.76}$ ( $0 \leq x \leq 0.5$ ) solid solution.	79
4.21	SEM micrographs of $(\text{Bi}_{3.36}\text{Mg}_{0.64-x}\text{Sr}_x)(\text{Mg}_{1.28}\text{Nb}_{2.72})\text{O}_{13.76}$ ( $0 \leq x \leq 0.5$ ) pyrochlores recorded at 3 k magnification.	81
4.22	The grains size distribution of $(\text{Bi}_{3.36}\text{Mg}_{0.64-x}\text{Sr}_x)(\text{Mg}_{1.28}\text{Nb}_{2.72})\text{O}_{13.76}$ ( $0 \leq x \leq 0.5$ ) pyrochlores.	82
4.23	Comparison of crystallite sizes between Scherrer, Williamson-Hall methods and internal strains of $(\text{Bi}_{3.36}\text{Mg}_{0.64-x}\text{Sr}_x)(\text{Mg}_{1.28}\text{Nb}_{2.72})\text{O}_{13.76}$ ( $0 \leq x \leq 0.5$ ) pyrochlores.	83
4.24	Williamson-Hall plot with five intense X-ray diffraction planes.	84
4.25	Arrhenius conductivity plots of $(\text{Bi}_{3.36}\text{Mg}_{0.64-x}\text{Sr}_x)(\text{Mg}_{1.28}\text{Nb}_{2.72})\text{O}_{13.76}$ ( $0 \leq x \leq 0.5$ ) cubic pyrochlores.	86
4.26	Complex impedance Cole-Cole plots of $(\text{Bi}_{3.36}\text{Mg}_{0.64-x}\text{Sr}_x)(\text{Mg}_{1.28}\text{Nb}_{2.72})\text{O}_{13.76}$ ( $0 \leq x \leq 0.5$ ) measured at different temperatures.	87
4.27	Combined spectroscopic plots of $\text{Bi}_{3.36}\text{Mg}_{1.52}\text{Sr}_{0.4}\text{Nb}_{2.72}\text{O}_{13.76}$ .	87
4.28	Plot of imaginary part of impedance as a function of frequency at different temperatures for composition, $\text{Bi}_{3.36}\text{Mg}_{1.52}\text{Sr}_{0.4}\text{Nb}_{2.72}\text{O}_{13.76}$ .	88
4.29	Combine plots of Arrhenius conductivity and peak frequency plot of $\text{Bi}_{3.36}\text{Mg}_{1.52}\text{Sr}_{0.4}\text{Nb}_{2.72}\text{O}_{13.76}$ .	88
4.30	Temperature dependence of dielectric constants of BMSN pyrochlores at 1 MHz.	90
4.31	Temperature dependence of dielectric losses of BMSN pyrochlores at 1 MHz.	90
4.32	The dielectric properties of BMSN pyrochlores at 25 °C and 1 MHz (a) temperature coefficient of capacitance, (b) dielectric losses and (c) dielectric constants.	91
4.33	XRD patterns of BMBN pyrochlores sintered at 1025 °C for 24 h.	93
4.34	The existence of forbidden peak (442) diffraction plane.	93
4.35	Variations of lattice parameter as a function of composition in BMBN pyrochlores.	95
4.36	TGA thermograms of BMBN solid solution.	97

4.37	DTA thermograms of BMBN solid solution.	97
4.38	IR spectra of BMBN solid solution.	99
4.39a	SEM micrographs of BMBN pyrochlores recorded at magnification of 3 k.	101
4.39b	Grain size distribution BMBN pyrochlores.	102
4.40	Williamson-Hall plot of five intense X-ray diffraction planes.	103
4.41	Comparison of crystallite sizes between Scherrer, Williamson-Hall methods and internal strains of BMBN pyrochlores.	104
4.42	Arrhenius conductivity plots of BMBN solid solution.	105
4.43	Complex impedance Cole-Cole plots of BMBN solid solution at 550 °C.	106
4.44	Combined spectroscopic plots of $\text{Bi}_{3.36}\text{Mg}_{1.72}\text{Ba}_{0.2}\text{Nb}_{2.72}\text{O}_{14.36}$ .	107
4.45	Plot of imaginary part of impedance, $Z''$ as a function of frequency at different temperatures for composition, $\text{Bi}_{3.36}\text{Mg}_{1.72}\text{Ba}_{0.2}\text{Nb}_{2.72}\text{O}_{14.36}$ .	108
4.46	Temperature dependence of dielectric constant, $\epsilon'$ of BMBN pyrochlores at fixed 1 MHz.	109
4.47	Temperature dependence of dielectric loss, $\tan \delta$ of BMBN pyrochlores at fixed 1 MHz.	109
4.48	Dielectric properties of BMBN pyrochlores at 25 °C and 1 MHz (a) temperature coefficient of capacitance (TCC), (b) dielectric losses ( $\tan \delta$ ) and (c) dielectric constants ( $\epsilon'$ ).	111
4.49	Cyclic voltammograms of (a) $\text{Bi}_{3.36}\text{Mg}_{1.92}\text{Nb}_{2.72}\text{O}_{13.76}$ , (b) $\text{Bi}_{3.36}\text{Mg}_{1.22}\text{Ca}_{0.7}\text{Nb}_{2.72}\text{O}_{13.76}$ , (c) $\text{Bi}_{3.36}\text{Mg}_{1.42}\text{Sr}_{0.5}\text{Nb}_{2.72}\text{O}_{13.76}$ and (d) $\text{Bi}_{3.36}\text{Mg}_{1.72}\text{Ba}_{0.2}\text{Nb}_{2.72}\text{O}_{14.36}$ pyrochlores.	113
4.50a	Specific capacitance of $\text{Bi}_{3.36}\text{Mg}_{1.92-x}\text{Ca}_x\text{Nb}_{2.72}\text{O}_{13.76}$ ( $0 \leq x \leq 0.7$ ) pyrochlores as a function of scan rate at 4, 20, 50, 100 and 200 $\text{mV s}^{-1}$ .	114
4.50b	Specific capacitance of $\text{Bi}_{3.36}\text{Mg}_{1.92-x}\text{Sr}_x\text{Nb}_{2.72}\text{O}_{13.76}$ ( $0 \leq x \leq 0.5$ ) pyrochlores as a function of scan rate at 4, 20, 50, 100 and 200 $\text{mV s}^{-1}$ .	115
4.50c	Specific capacitance of $\text{Bi}_{3.36}\text{Mg}_{1.92-x}\text{Ba}_x\text{Nb}_{2.72}\text{O}_{14.36}$ ( $0 \leq x \leq 0.2$ ) pyrochlores as a function of scan rate at 4, 20, 50, 100 and 200 $\text{mV s}^{-1}$ .	115

4.51	Galvanostatic charge-discharge curves of BMN pyrochlore investigated in 1.0 M KCl at various current densities: (a) 0.00004 A g <sup>-1</sup> , (b) 0.00005 A g <sup>-1</sup> , (c) 0.00006 A g <sup>-1</sup> , (d) 0.00007 A g <sup>-1</sup> and (e) 0.00008 A g <sup>-1</sup> .	117
4.52a	Specific capacitance against current density of Bi <sub>3.36</sub> Mg <sub>1.92</sub> Nb <sub>2.72</sub> O <sub>13.76</sub> pyrochlore by 1-, 3- and 5-layer.	119
4.52b	Specific capacitance against current density of Bi <sub>3.36</sub> Mg <sub>1.92-x</sub> Ca <sub>x</sub> Nb <sub>2.72</sub> O <sub>13.76</sub> (x = 0.1) pyrochlore by 1-, 3- and 5-layer.	119
4.52c	Specific capacitance against current density of Bi <sub>3.36</sub> Mg <sub>1.92-x</sub> Ca <sub>x</sub> Nb <sub>2.72</sub> O <sub>13.76</sub> (x = 0.3) pyrochlore by 1-, 3- and 5-layer.	120
4.52d	Specific capacitance against current density of Bi <sub>3.36</sub> Mg <sub>1.92-x</sub> Ca <sub>x</sub> Nb <sub>2.72</sub> O <sub>13.76</sub> (x = 0.5) pyrochlore by 1-, 3- and 5-layer.	120
4.52e	Specific capacitance against current density of Bi <sub>3.36</sub> Mg <sub>1.92-x</sub> Ca <sub>x</sub> Nb <sub>2.72</sub> O <sub>13.76</sub> (x = 0.7) pyrochlore by 1-, 3- and 5-layer.	121
4.52f	Specific capacitance against current density of Bi <sub>3.36</sub> Mg <sub>1.92-x</sub> Sr <sub>x</sub> Nb <sub>2.72</sub> O <sub>13.76</sub> (x = 0.1) pyrochlore by 1-, 3- and 5-layer.	121
4.52g	Specific capacitance against current density of Bi <sub>3.36</sub> Mg <sub>1.92-x</sub> Sr <sub>x</sub> Nb <sub>2.72</sub> O <sub>13.76</sub> (x = 0.3) pyrochlore by 1-, 3- and 5-layer.	122
4.52h	Specific capacitance against current density of Bi <sub>3.36</sub> Mg <sub>1.92-x</sub> Sr <sub>x</sub> Nb <sub>2.72</sub> O <sub>13.76</sub> (x = 0.5) pyrochlore by 1-, 3- and 5-layer.	122
4.52i	Specific capacitance against current density of Bi <sub>3.36</sub> Mg <sub>1.92-x</sub> Ba <sub>x</sub> Nb <sub>2.72</sub> O <sub>14.36</sub> (x = 0.1) pyrochlore by 1-, 3- and 5-layer.	123
4.52j	Specific capacitance against current density of Bi <sub>3.36</sub> Mg <sub>1.92-x</sub> Ba <sub>x</sub> Nb <sub>2.72</sub> O <sub>14.36</sub> (x = 0.2) pyrochlore by 1-, 3- and 5-layer.	123
4.53a	Galvanostatic charge-discharge curve for Bi <sub>3.36</sub> Mg <sub>1.92-x</sub> Ca <sub>x</sub> Nb <sub>2.72</sub> O <sub>13.76</sub> (0 ≤ x ≤ 0.7) pyrochlores.	127
4.53b	Galvanostatic charge-discharge curve for Bi <sub>3.36</sub> Mg <sub>1.92-x</sub> Sr <sub>x</sub> Nb <sub>2.72</sub> O <sub>13.76</sub> (0 ≤ x ≤ 0.5) pyrochlores.	127
4.53c	Galvanostatic charge-discharge curve for Bi <sub>3.36</sub> Mg <sub>1.92-x</sub> Ba <sub>x</sub> Nb <sub>2.72</sub> O <sub>14.36</sub> (0 ≤ x ≤ 0.2) pyrochlores.	128
4.54a	Specific capacitance of Bi <sub>3.36</sub> Mg <sub>1.92-x</sub> Ca <sub>x</sub> Nb <sub>2.72</sub> O <sub>13.76</sub> (0 ≤ x ≤ 0.7) pyrochlores as a function of current density.	128
4.54b	Specific capacitance of Bi <sub>3.36</sub> Mg <sub>1.92-x</sub> Sr <sub>x</sub> Nb <sub>2.72</sub> O <sub>13.76</sub> (0 ≤ x ≤ 0.5) pyrochlores as a function of current density.	129
4.54c	Specific capacitance of Bi <sub>3.36</sub> Mg <sub>1.92-x</sub> Ba <sub>x</sub> Nb <sub>2.72</sub> O <sub>14.36</sub> (0 ≤ x ≤ 0.2) pyrochlores as a function of current density.	129

pyrochlores as a function of current density.

- 4.55a Nyquist plot of  $\text{Bi}_{3.36}\text{Mg}_{1.92-x}\text{Ca}_x\text{Nb}_{2.72}\text{O}_{13.76}$  ( $0 \leq x \leq 0.7$ ) 131  
pyrochlore thin films in the frequency range 1 MHz to 1 Hz. Inset  
is the equivalent circuit.
- 4.55b Nyquist plot of  $\text{Bi}_{3.36}\text{Mg}_{1.92-x}\text{Sr}_x\text{Nb}_{2.72}\text{O}_{13.76}$  ( $0 \leq x \leq 0.5$ ) 131  
pyrochlore thin films in the frequency range 1 MHz to 1 Hz. Inset  
is the equivalent circuit.
- 4.55c Nyquist plot of  $\text{Bi}_{3.36}\text{Mg}_{1.92-x}\text{Ba}_x\text{Nb}_{2.72}\text{O}_{14.36}$  ( $0 \leq x \leq 0.2$ ) 132  
pyrochlore thin films in the frequency range 1 MHz to 1 Hz. Inset  
is the equivalent circuit.





## LIST OF ABBREVIATIONS

3D	three dimensions
AC	alternating current
ATR	attenuated total reflectance
CD	galvanostatic charge-discharge
CRT	cathode ray tube
CV	cyclic voltammetry
DTA	differential thermal analysis
EC	electrochemical capacitor
EDS	energy dispersive spectroscopy
EIS	electrochemical impedance spectroscopy
FT-IR	fourier transform infrared spectroscopy
FTO	fluorine-doped tin oxide
FWHM	Full width at half maximum
HTCC	high temperature co-fired ceramics
ICDD	international centre for diffraction data
ICP-OES	inductive-coupled plasma optical emission spectroscopy
ITO	indium tin oxide
LTCC	low temperature co-fired ceramics
MGC	multiplayer glass-ceramics
MLC	multi-layered ceramic
MLCC	multilayer ceramic capacitor
MOD	metalorganic decomposition
ppm	parts per million
rf	radio frequency



RR	radius ratio
SC	specific capacitance
SEAD	selected electron area diffraction
SEM	scanning electron microscopy
TCC	temperature coefficient of capacitance
TC $\epsilon$ '	temperature coefficient of permittivity
TGA	thermogravimetric analysis
W-H	Williamson and Hall
XRD	x-ray diffraction
XRF	x-ray fluorescence
$\theta$	Bragg angle
A	area
$a, b, c, \alpha, \beta, \gamma$	lattice parameters
C	capacitance
$c$	velocity of light
C <sub>b</sub>	bulk capacitance
C <sub>gb</sub>	grain boundary capacitance
C <sub>o</sub>	vacuum capacitance
d	d-spacing
$d$	distance
$E$	electric field
E <sub>a</sub>	activation energy
eV	electron volt
$I$	current
K	kelvin
$k_B$	Boltzmann's constant

$M^*$	complex electric modulus
$M'$	real part of electric modulus
$M''$	imaginary part of electric modulus
$n$	carrier concentration
$P$	Polarisation
$Q$	charge
$Q_0$	vacuum charge
$R$	resistance
$R_b$	bulk resistance
$\tan \delta$	dielectric loss
$V$	voltage
$Y^*$	complex admittance
$Y'$	real part of admittance
$Y''$	imaginary part of admittance
$Z^*$	complex impedance
$Z'$	real part of impedance
$Z''$	the imaginary part of impedance
$\alpha$	conductivity
$\alpha_c$	temperature coefficient of dielectric constant
$\alpha_e$	electronic polarisability
$\alpha_i$	ionic polarisation
$\alpha_o$	orientation polarisation
$\varepsilon$	strain
$\varepsilon'$	real part of permittivity
$\varepsilon''$	imaginary part of permittivity

$\epsilon_0$	free space
$\epsilon_r$	relative permittivity
$\lambda$	wavelength
$\mu$	carrier mobility
$\tau_c$	tunable temperature coefficients of capacitance
$\phi$	phase
$\chi$	susceptibility
$\omega$	angular frequency



© COPYRIGHT UPM

# CHAPTER 1

## INTRODUCTION

### 1.1 The Fundamental of Ceramic

Ceramic, is also recognised as *keromos* (Greek) in ancient times originating from clay of potter which is able to be fired in the temperature range of 900–1200 °C. Clay is mouldable when it is still wet and able to retain its shape after drying and firing. After experiencing a few evolutions, clay can be converted into ceramics with outstanding mechanical and electrical properties once it is fired at appropriate high temperature. In other perspective of solid description, ceramic is a polycrystalline, inorganic and non-metallic material that gains mechanical strength through firing or sintering process regardless of it is an amorphous or single crystal (Moulson and Herbert, 2003).

#### 1.1.1 Electroceramics

The research in electroceramics has been critically driven by the great demand in technology and device applications that widely used in energy conversion and storage, health care, electronics and communication devices and automobile transportation.

A great interest and effort has been focused on the field of electroceramic over last few decades, several subclasses of electroceramics arise in parallel with the growth of technology advancement. For example, high dielectric capacitance and consistent memories of ferroelectric materials, outstanding energy storage and conversion of solid electrolyte materials, as well as environment monitoring of semiconducting oxides are prominent for a wide range of applications. The different types of electroceramics including: (i) ceramic conductors, (ii) ionic conductor, (iii) ceramic insulators, (iv) magnetic ceramics and (v) optical ceramics.

The relative mobility of electrons within a material is known as electric conductivity. Materials with the high electron mobility are called conductors. Conductive ceramics are one of the conductors and are capable to sustain their mechanical integrity at high temperature above 1500 °C. Ceramic conductors are excellent of electricity and most of these conductors are advanced ceramics materials whose properties are modified through precise control over their fabrication from powders into products. Table 1.1 shows a list of some ceramic conductor materials used in different applications (Moulson and Herbert, 2003).

**Table 1.1: List of some ceramic conductor materials used in different applications** (Moulson and Herbert, 2003).

Application	Materials
Resistors and Electrodes	PbO, RuO <sub>2</sub> , BiRu <sub>2</sub> O <sub>7</sub> , SnO <sub>2</sub>
Thermistor	BaTiO <sub>4</sub>
Heating element	SiC, MoSi <sub>2</sub> , ZrO <sub>2</sub>
Chemical Sensors	ZrO <sub>2</sub> , Al <sub>2</sub> O <sub>3</sub> , β-Al <sub>2</sub> O <sub>3</sub> , SnO <sub>2</sub> , Nasicon, TiO <sub>2</sub> , SrTiO <sub>4</sub> , etc.
Fuel cells	Y <sub>2</sub> O <sub>3</sub> -ZrO <sub>2</sub>
Batteries	β-Al <sub>2</sub> O <sub>3</sub> , Nasicon, Lasicon
Ceramic Capacitors	BaTiO <sub>3</sub> , PZT [Pb(Zr, Ti)O <sub>2</sub> ]

In ionic conductors, the current are transported by ions moving through the crystal lattice. The electrical current transports through ions in conducting liquid are called as electrolytes whereas ion conducting solids are known as solid electrolytes. The conductivity values in ionic conductors for liquid electrolyte materials and solid electrolyte materials are in the range of  $10^{-1}$ – $10^3$  Sm<sup>-1</sup> and  $10^{-1}$ – $10^3$  Sm<sup>-1</sup>, respectively. Whilst, the factors that influencing the conductivity values,  $\alpha$  are (i) carrier concentration,  $n$ , (ii) carrier mobility,  $\mu$  and (iii) charge of carriers,  $Z$  as formulated in equation below:

$$\alpha = nZe\mu \quad (1.1)$$

**Table 1.2: List of few conductive ceramic materials used as solid electrolytes in sensor to sense different elements and compounds** (Moulson and Herbert, 2003).

Solid Electrolyte	Elements/Compounds
Stabilised ZrO <sub>2</sub>	Oxygen
Sulfur	CaS, CaF <sub>2</sub> , β-Alumina, Nasicon
Stabilised ZrO <sub>2</sub> , K <sub>2</sub> SO <sub>4</sub> , Na <sub>2</sub> SO <sub>4</sub> , Li <sub>2</sub> SO <sub>4</sub> , β-Alumina and Nasicon	SO <sub>x</sub> (x = 2.3)
Stabilised ZrO <sub>2</sub>	NO <sub>x</sub> (x = 1.2)
Stabilised ZrO <sub>2</sub> , K <sub>2</sub> SO <sub>4</sub> and Na <sub>2</sub> SO <sub>4</sub>	CO <sub>x</sub> (x = 1.2)

In contrast to conductors, insulators are materials that impede the free flow of electrons from atom to atom, offering very large resistance to the flow of electric current. Some materials are particularly good insulators and can be characterised by their high resistivities, e.g. glass, mica and quartz (fused) having their resistivity value of  $10^{12}$ ,  $9 \times 10^{13}$  and  $5 \times 10^{16}$  ohm m, respectively. The materials generally used for insulating purpose are called as insulating materials which have some specific properties: (i) it must be mechanically strong enough to carry tension and weight of conductors, (ii) it must have very high dielectric strength to withstand the voltage stresses in high voltage system, (iii) it must possess high insulation resistance to prevent leakage current to the earth, (iv) the insulating material must be free from undesired impurities, (v) it should not be porous, (vi) there must not be any entrance on the surface of electrical insulator so that the moisture or gases can enter in it and (vii) the physical as well as electrical properties must be less affected by changing temperature. The materials with the insulating components based on natural minerals include porcelains (clay-based and

talc-based), alumina, beryllia, glass, polymer insulators, aluminium nitride and ceramic ‘packaging’ technology (Moulson and Herbert, 2003).

Over the past decade, ceramic magnets have been firmly established as electrical and electronic engineering materials; containing iron as a major constituent and are known collectively as ‘ferrites’. Ampere, Biot, Savart and Oersted were among the first to demonstrate that conductors carrying currents produced magnetic fields and exerted ‘Lorentz’ forces on each other (Barsoum, 2003). Magnetic ceramics possess excellent properties, e.g. strong magnetic coupling, low loss characteristics and high electrical resistivity and these features help to create new devices for applications in data storage, tunnel junctions, high frequency applications and spin valves. Magnetic materials can be identified based on magnetic susceptibility values. Materials with negative susceptibility ( $\chi_m < 1$ ) are diamagnetic which show very insignificant negative susceptibility value. Superconductor in superconducting state exhibiting  $\chi_m = -1$ , which is very useful for magnetic levitation applications. However, materials with  $\chi_m > 1$  are either paramagnetic (small positive susceptibility value) or ferromagnetic (large positive susceptibility value) (Moulson and Herbert, 2003). Table 1.3 shows the different types of magnetism with the susceptibility value of some materials.

**Table 1.3: Different types of magnetism with the susceptibility value of some materials** (Moulson and Herbert, 2003).

Type of Magnetism	Material	$\chi$ (SI) unitless	$\chi$ (cgs) unitless	$\mu$ unitless
Diamagnetic	Cu	$-9.7 \times 10^{-6}$	$-0.77 \times 10^{-6}$	0.99999
	Si	$-4.1 \times 10^{-6}$	$-0.32 \times 10^{-6}$	0.99999
Paramagnetic	Al	$+20.7 \times 10^{-6}$	$+1.65 \times 10^{-6}$	1.00002
	Pt	$+264.4 \times 10^{-6}$	$+21.04 \times 10^{-6}$	1.000026
Ferromagnetic	Low carbon steel	$\approx 5 \times 10^3$	$3.98 \times 10^2$	$5 \times 10^3$
	Fe-3%Si (Grain Oriented)	$4 \times 10^3$	$3.18 \times 10^3$	$4 \times 10^4$

Diamagnetic materials are materials having electron motions in the way of those electrons produce net zero magnetic moment in the absence of any magnetic field (Goldman, 2006).

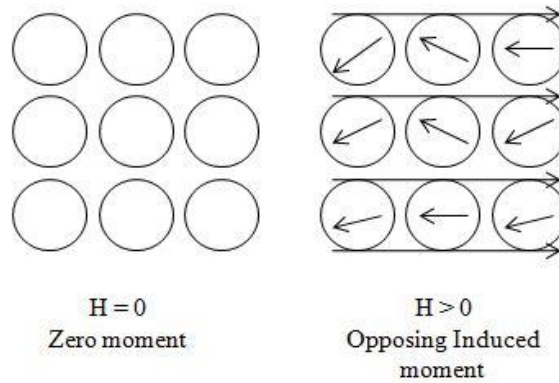


**Figure 1.1: Description of a diamagnetic material in the absence of a magnetic field and when a field is applied** (Goldman, 2006).

In paramagnetic materials, atoms possess a permanent non-zero net magnetic moment owing to factor of orbital and spin magnetic moments. However, once magnetic field is applied, magnetic moment would align up in the direction of magnetic field overcoming thermal barrier and creating a positive magnetic moment with small susceptibilities,  $10^{-3}$  to  $10^{-6}$  (Riedel and Chen, 2014).

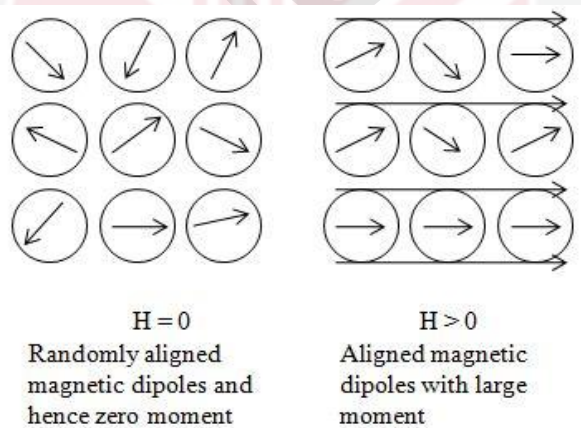


**Figure 1.2: Schematic diagram of spins in a paramagnetic solid** (Riedel and Chen, 2014).

Ferromagnetic materials are quite similar to paramagnetic materials in term of having permanent magnetic moment, but ferromagnetic materials have its regions or domains in ordered and aligned that give rise to large finite magnetisation in the absence of magnetic field. When magnetic field is applied, ferromagnetic materials exhibit a ferroelectric-like hysteresis loop between magnetisation and magnetic field as below.



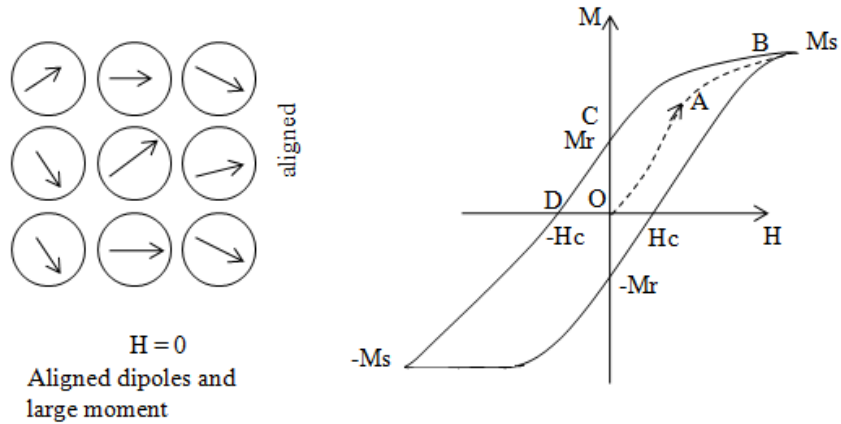


**Figure 1.3: Schematic diagram of spins in a ferromagnetic material and ferromagnetic hysteresis loops (Riedel and Chen, 2014).**

Optical ceramics, also known as transparent ceramics is a great substitution of single crystal due to several reasons, e.g. cost effectiveness, large-scale production, feasibility of shape controlling and better mechanical properties. Unlike single crystal, transparent ceramics have various sites to scatter light, e.g. residual pores within grains and grain boundaries, grain boundaries, second phase at the grain boundaries and double refraction from birefringent materials. The most critical factor for transparency of the ceramics is porosity. The presence of a large number of pores makes the ceramic opaque (non-transparent). Transparent ceramics contain both grains and grain boundaries. If there is a deviation in properties such as composition between grains and grain boundaries, the interfaces between them would be the scattering sites of light. Thus, the difference in optical characteristic between grains and grain boundaries should be minimised in order to keep ceramic transparent (Kong *et al.*, 2015). For example, the transparent ceramics,  $\alpha$ -alumina ( $\text{Al}_2\text{O}_3$ ) or addressed as corundum is the only thermodynamically stable crystallographic modification of alumina. Corundum has its  $\text{O}^{2-}$  ions arranged in hexagonal arrangement with  $\text{Al}^{3+}$  occupying two-thirds of the octahedral interstitial position in hexagonal crystal lattice. Corundum exhibits maleficent properties, e.g. high strength, high hardness, and excellent corrosive resistance, making corundum a promising and favourable candidate for applications in electromagnetic windows, transparent armor and envelopes of high pressure metal halide lamps (Kong *et al.*, 2015).

In the near future, electroceramic materials will be a favourable choice to be intensively integrated in many ways of virtual design to fit into this evolution especially through miniaturisation of conventional semiconducting, superconducting and ironically conducting materials without losing or degrading the potential properties (Setter and Waser, 2000).



## 1.2 Dielectric Materials

Dielectrics or electrically insulated materials are defined as a class of materials in which electrostatic fields could hold for a long time, offering a very high resistance to electric current flow. Thus, dielectrics materials are always a favourable choice of a wide spectrum of applications including devices of energy storage in capacitors, charge storage in photosensitive materials of printers and copying machines, transducers in condenser and piezoelectric microphone, liquid crystals for alphanumeric displays and other display usages (Murarka *et al.*, 2003; Ho *et al.*, 2002).

Dielectric materials typically are not utilised to pass electrical energy via conduction, yet they could become a media transferring electrical energy through displacement of current. Distinction of dielectric properties depending on composition, structure and experimental condition of the dielectric materials has been established since these are the key factors to be altered in order to satisfy the needs of different applications and to enhance the performance and reliability of dielectric materials. Thus, various dielectric properties are carefully deliberated especially the ability of reservation and dissipation of electric and magnetic energies, and degree of polarisation, magnetisation and conduction (Jack and George, 1979).

### 1.2.1 Dielectric Constant

Dielectric constant, also addressed as relative permittivity,  $\epsilon'$ , is one of the chief factors to be regarded in designing the performance of dielectric material during practical applications. Dielectric constant defines the ability of material to concentrate electrostatic flux or to store electrical energy in the presence of an electric field (Bartnikas, 1987).

There are a few categories of dielectric material depending on the magnitude of dielectric constant, which are low, medium and high permittivity classes. High permittivity dielectric materials, e.g. BaTiO<sub>3</sub> could be a great substitution for mica in capacitors. Meanwhile, titanium oxide could be used to modify medium and low permittivity classes especially for the low-loss stable capacitors and microwave capacitors. The ceramic insulators include silicates and aluminas that used to be utilised as ceramic insulating purposes (Nanni *et al.*, 1999).

Dielectric constant can be described as a comparison between permittivity of a medium and permittivity of free space as formulated below:

$$\epsilon_r = \epsilon/\epsilon_0 \quad (1.2)$$

All materials, inclusive vacuum, do store energy when electric field applied. The permittivity of free space,  $\epsilon_0$  is a constant with value  $\epsilon_0 = 8.854 \times 10^{-12} \text{ Fm}^{-1}$ . Apparently, capacitor materials are not all originated from free space, thus  $\epsilon$  is the absolute permittivity of a medium and  $\epsilon_r$  is the relative permittivity which has a value always

greater than 1, representing all materials are able to store more electrical energy than free space in the presence of electric field (Nalwa, 1999).

### 1.2.1.1 Polarisation

When a potential difference,  $V$  is applied between two parallel electrodes that having an area of cross section,  $A$  m<sup>2</sup> and distance,  $d$  m apart in a vacuum capacitor, the electric field,  $E$  between the electrodes perpendicular to the plates, regardless edge effect, (Raju, 2009).

$$E = V / d \quad (1.3)$$

Thus, the capacitance of vacuum capacitor is:

$$C_0 = \epsilon_0 A / d \quad (1.4)$$

Moreover, charge captured in the vacuum capacitor is then becomes:

$$Q_0 = \epsilon_0 A E \quad (1.5)$$

where  $\epsilon_0$  is the permittivity of free space.

Homogenous dielectric leads to potential constant, and charge stored is then formulated as:

$$Q = \epsilon_0 \epsilon A E \quad (1.6)$$

where  $\epsilon$  is the dielectric constant of the material (permittivity of the medium).

Apparently,  $\epsilon$  is always greater than unity and  $Q$  is greater than  $Q_0$ , a raise in charge stored due to appearance of charges on the dielectric surface, is described as:

$$Q - Q_0 = A E \epsilon_0 (\epsilon - 1) \quad (1.7)$$

If charges in the system are neutral, dipole moment is created as:

$$\mu = A E \epsilon_0 (\epsilon - 1) d \quad (1.8)$$

Since volume of dielectric is  $v = A d$ , then dipole moment per unit volume is:

$$\mu / A d = E \epsilon_0 (\epsilon - 1) \quad (1.9)$$

Polarisation,  $P$  is defined as the dipole moment per unit volume and expressed as:

$$P = E\epsilon_0 (\epsilon - 1) \quad (1.10)$$

$$P = \chi E\epsilon_0 \quad (1.11)$$

where  $\chi$  is  $(\epsilon - 1)$  which is known as susceptibility of medium.

In short, polarisation is defined as a vector quantity of the dielectric dipole moment per unit volume regarding magnitude and direction. Yet, polarisation is charge per unit area on the surface of dielectric material in the absence of electric field (Kim and Tadokoro, 2007).

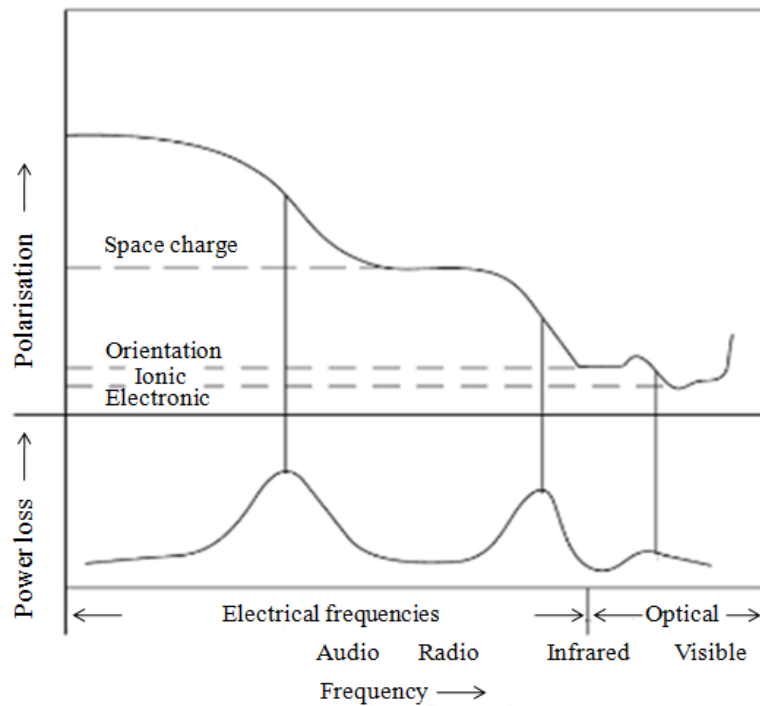


**Figure 1.4: Frequency dependence of polarisation processes and peak power losses** (Kim and Tadokoro, 2007).

### 1.2.1.1.1 Electronic Polarisation

In the existence of external electric field, a slightly displacement occurs between positive charged nucleus and negative electron cloud in the way of positive charged nucleus stays in direction of electric field and negative electron cloud sits in opposite direction, Consequently, positive nucleus is no longer at centroid of electronic charge, thus resulting electronic polarisation. Electronic polarisation has a small magnitude of

polarisation because the external electric field applied is usually weak compared with intra-atomic field (Kim and Tadokoro, 2007).

Electronic polarisation is proportional to the magnitude of field strength formulated as below:

$$P_e = \alpha_e E \quad (1.12)$$

where  $\alpha_e$  is the electronic polarisability constant in which  $\alpha_e$  increases when atom becomes larger, and  $\alpha_e$  is independent of temperature since electronic structure of an atom is insensitive towards temperature. In addition,  $\alpha_e$  is also independent of frequency due to electronic polarisation occurs within extremely short time ( $\sim 10^{-15}$  to  $\sim 10^{-14}$  seconds).

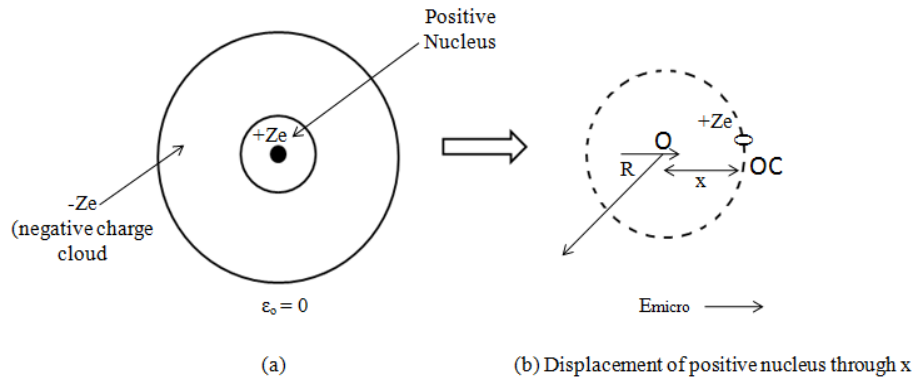


**Figure 1.5: The total negative charge  $-Ze$  is distributed homogeneously throughout the sphere of  $R$  (a) while the nucleus and electron cloud are displaced in opposite direction (b) (Maheshwari, 2006).**

#### 1.2.1.1.2 Ionic Polarisation

Ionic polarisation happens owing to displacement of the atomic components of the molecule in electric field when atoms transform to molecules. During the transformation to molecules, electron clouds of atoms do not distribute their electron symmetrically or evenly since electron clouds tend to stay towards atoms with higher electronegativity. Thus, molecules formation requires atoms with charges of opposite polarity. With application of external electric field, net charges alter the equilibrium position of atoms themselves, resulting ionic polarisation which has a smaller polarisation magnitude, approximately one-tenth of electronic polarisation (Ganeswara-Rao, 2008; Marikani, 2017).

$$P_i = \alpha_i E \quad (1.13)$$

where  $\alpha_i$  is the ionic polarisation constant in which  $\alpha_i = 0.1\alpha_e$  due to greater mass of ions ( $\sim 10^{-13}$ ), and  $\alpha_i$  is independent of temperature because molecular structure and electron distribution in molecule are insensitive of both temperature and frequency.

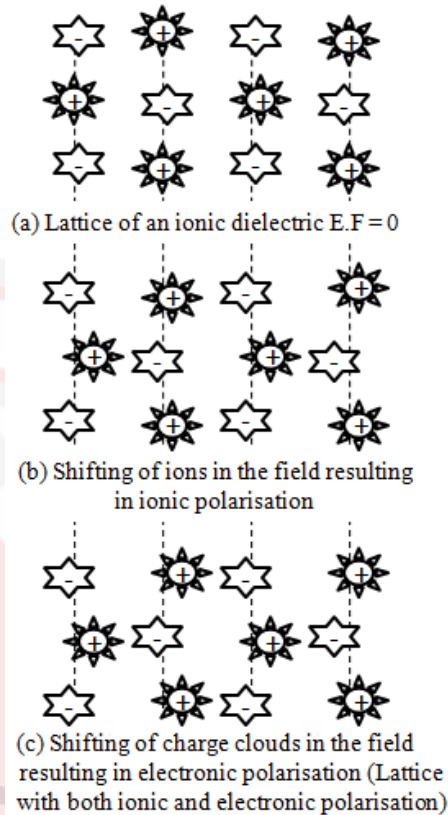


**Figure 1.6: Ionic polarisation measures shift of ions relative to each other and electronic polarisation measures shift of electron cloud relative to nucleus within the atom (Maheshwari, 2006).**

### 1.2.1.1.3 Orientational Polarisation

Organic molecules, e.g.  $\text{CH}_3\text{Cl}$ ,  $\text{H}_2\text{O}$  and  $\text{HCl}$  in general have significant difference in electronegativity between the positive and negative partial charge and this could create dipoles moment in the absence of electric field. Dipole moment shown is negligibly small since molecules dipoles are oriented randomly without existence of electric field. With the aid of electric field, orientation of dipoles is arranged in the direction of electric field resulting in vast dipole moments (Mitchell, 2004; Marikani, 2017).

$$P_o = \alpha_o E \quad (1.14)$$

where  $\alpha_o$  is the orientation polarisation constant in which  $\alpha_o$  is dependent on temperature and  $\alpha_o$  decreases with increase in temperature due to thermal energy of high temperature is able to disorient the dipoles.

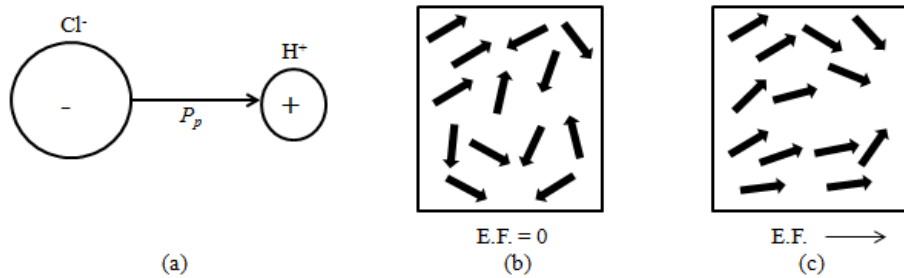


**Figure 1.7: Orientation polarisation produced in the case of a polar molecule of an electric field (Maheshwari, 2006).**

#### 1.2.1.1.4 Space Charge Polarisation

Charge carriers commonly exist in heterogeneous systems where charge carriers can migrate through material under the effect of external electric field. However, when the charge carriers have its motion obstructed, charge carriers are confined at defect sites or at interface between medium that have dissimilar dielectric constant and conductivity, thus hindering the movement of charge carriers in discharging or replacing at the electrodes. Consequently, inhibition of charge carrier movement leads to space charge of macroscopic field distortion (Martin *et al.*, 2009; Macdonald, 1953).

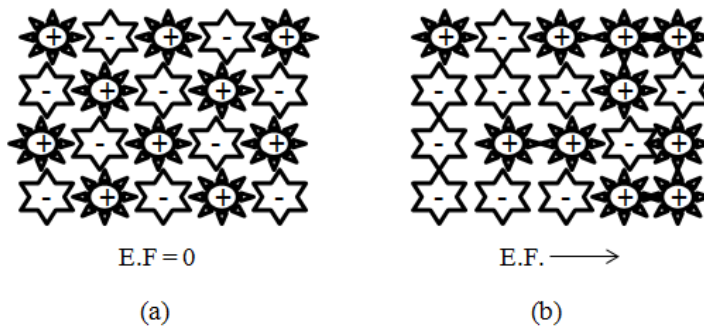


**Figure 1.8: Space charge polarisation (Maheshwari, 2006).**

#### 1.2.2 Dielectric Loss

Dielectric loss, or dissipation factor is meant to display deviation from ideal behavior of a dielectric material, or defined as quantitatively dissipation of the electrical energy due to various physical processes, e.g. electrical conduction, dielectric relaxation,

dielectric resonance and losses besides a typical loss comes from a delay between electric field and electric displacement vector (Sawada *et al.*, 1999). Dielectric loss can be branched into intrinsic and extrinsic loss. Intrinsic losses are the losses in a perfect crystal depending on the crystal structure, and significantly due to dielectric relaxation in ideal lattice at low frequency that leads to release of heat. Extrinsic losses are attributed by imperfections in a crystal structure due to the presence of impurities, microstructural defects, porosity, grain boundaries, dislocations and vacancies (Sebastian, 2008).

$$\tan \delta = \epsilon''/\epsilon' \quad (1.15)$$

The equation above illustrates ratio of the imaginary permittivities to the real storage relative permittivities or can also be explained as ratio of the energy dissipated to energy stored in material. The tangent of the loss angle is present when a dielectric is susceptible to a sinusoidally varying applied electric field. Ordinarily, dielectric loss is determined experimentally using same method as the procedure used to find dielectric constant concurrently. Dielectric loss is affected by temperature and frequency, until a maximum value of dielectric relaxation is overcome (Alger, 1997).

### 1.2.3 Temperature Coefficient of Capacitance (TCC)

Temperature coefficient of capacitance (TCC) is the maximum change in capacitance over a specific temperature range. The capacitance value stated by the manufacturer is established at a reference temperature range of ~30 °C to ~300 °C. TCC should always be considered for applications operating above or below this temperature. For class I capacitors, they are highly stable with temperature and are referred to as temperature compensating. It is always specified as the capacitance change in parts per million (ppm) per degrees centigrade, and the maximum capacitance change is calculated via formula below:

$$TCC = (C_f - C_i) 1,000,000 / (T_f - T_i) C_i \quad (1.16)$$

where  $C_f$  and  $C_i$  is the capacitance value at initial temperature,  $T_i$  (~30 °C) and final temperature  $T_f$  (~300 °C) respectively.

Meanwhile, for class II capacitors, it is different from class I which is not the temperature stable but having the main advantage in volumetric efficiency, e.g. in the case involving more capacitance. This capacitors are best suited for applications where higher capacitance values are important while charge  $Q$  and stability over temperature are not of major concern. Temperature coefficient of capacitance for class II capacitor dielectrics are expressed as a percentage. TCC should always be operating at temperature above or below 25 °C (Fiore, 2000).



### 1.3 Applications of Dielectric Ceramics

#### 1.3.1 Low Temperature Co-fired Ceramics (LTCC)

Material made up of low fraction of dielectric ceramic (3/1), is known as low temperature co-fired ceramics (LTCC) or can be called as multilayer glass-ceramics (MGC). LTCC material can be sintered at much lower firing temperature (850 °C to 900 °C) compared to high temperature co-fired ceramics (HTCC) that is sintered at high temperature around 1500 °C. Since LTCC can be produced at much lower temperature, low resistivity precious metal conductors, e.g. gold and silver can be used as the cathode materials of LTCC material to suit many electrical applications.

To satisfy the demand for new packaging technology that requires high frequency and high interconnect density material, new glass-ceramic materials with low dielectric constant are highly needed. Unlike alumina with high dielectric constant that is able to give a trouble in switching speed, silver and palladium in desired particle shape are preferred and needed as glass-ceramic substrate to fulfil the latest technology requirements: (i) new LTCC material with an insignificant propagation delay due to low dielectric constant material and (ii) low electrical resistivity and low cost of improved electrical design that helps to control characteristic impedance and crosstalk coupling noise (Christou, 2006).

**Table 1.4: Typical materials of low and high temperature co-fired ceramic systems (Christou, 2006).**

	Ceramics		Conductor	
	Material	Firing temperature (°C)	Material	Melting point (°C)
LTCC	<ul style="list-style-type: none"> <li>• Glass/Ceramic composite</li> <li>• Crystallised glass</li> <li>• Crystallised glass/Ceramic composite</li> <li>• Liquid-phase sintered ceramics</li> </ul>	900 to 1000	<ul style="list-style-type: none"> <li>Cu</li> <li>Au</li> <li>Ag</li> <li>Ag-Pd</li> <li>Ag-Pt</li> </ul>	<ul style="list-style-type: none"> <li>1083</li> <li>1063</li> <li>960</li> <li>960-1555</li> <li>960-1186</li> </ul>
HTCC	<ul style="list-style-type: none"> <li>• Alumina ceramics</li> </ul>	1600 to 1800	<ul style="list-style-type: none"> <li>Mo</li> <li>W</li> <li>Mo-Mn</li> </ul>	<ul style="list-style-type: none"> <li>2610</li> <li>3410</li> <li>1246-1500</li> </ul>

#### 1.3.2 Multilayer Ceramic Capacitors (MLCC)

Recently, ceramic capacitor has achieved the highest number in production and sales among fine ceramics products in a rapidly growth market. Multilayer ceramic capacitor (MLCC) has its demand raises remarkably year by year and reaches global output demand as high as 9 trillion units. The advancement of technology does not halt by just here, stringent requirements that demand high specific capacitance, high layer number with ultra-thin layer and cost effectiveness in the production. MLCCs can be found widely in applications ranging from military, spaceflight, communication to national



defence (Yin *et al.*, 2009). In the trend of miniaturisation of ceramic capacitors, MLCC layers are reduced from 10  $\mu\text{m}$  to 3  $\mu\text{m}$  and towards 1  $\mu\text{m}$ . Thus, MLCC ceramic grain size has to be controlled within nanoscale of 100 nm suggesting that grain growth needs to be suppressed during sintering process.

#### 1.4 Problem Statements

It is imperative to prepare novel pyrochlores with excellent electrical performance especially the complex family of pyrochlores has a wide range of compositions and electrical properties. By far, bismuth zinc niobate pyrochlores (BZN) and bismuth magnesium niobate pyrochlores (BMN) are well known to be used as dielectric materials that are applicable for technological devices and modules. Thus, the preparation of new BMN pyrochlore through chemical doping is expected to yield materials with high dielectric constant and low dielectric loss. The selection of these dopants is due to the reasons including: (i) larger ionic radius that suits the requirement of relatively larger A site, (ii) same oxidation state with  $\text{Mg}^{2+}$  and (iii) high polarisability of  $\text{Ca}^{2+}$ ,  $\text{Sr}^{2+}$  and  $\text{Ba}^{2+}$ , which is expected to enhance the dielectric properties. The idea of depositing Ca, Sr and Ba doped BMN pyrochlores on thin film in solid electrolyte systems by using electrochemical impedance spectroscopy method (EIS) is due to their vast applications as energy storage devices for electronic components, electric vehicles and memory back-up systems in mobile phone and computers. Utilisation of this technique has attracted the attention of worldwide researchers due to their excellent specific capacitance, e.g.  $\sim 59$  F/g and 123.8 F/g (Chang *et al.*, 2012b; Chee *et al.*, 2015) with a good electrochemical stability. By far, information and literature concerning the properties of pyrochlores in the doped BMN systems are rarely found. Therefore, control of composition, synthesis condition and chemical dopants is of utmost importance in order to synthesise new pyrochlores with improved electrical properties.

#### 1.5 Objectives

The objectives of this research are:

- i. To prepare chemically doped pyrochlores in the  $\text{Bi}_2\text{O}_3\text{-MgO-AO-Nb}_2\text{O}_5$  (A = Ca, Sr and Ba) ternary systems.
- ii. To study structural and thermal properties of the prepared pyrochlores.
- iii. To characterise the electrical behavior of the chemically doped BMN pyrochlores by AC impedance spectroscopy.
- iv. To investigate specific capacitance of pyrochlore thin films coated on indium tin oxide (ITO) glass using electrochemical impedance spectroscopy method (EIS).

## REFERENCES

- Abram, E.J., Sinclair, D.C. and West, A.R. 2001. Electrode-contact spreading resistance phenomena in doped-lanthanum gallate ceramics. *Journal of Electroceramics* 7(3): 179–188.
- Alger, M. 1997. Dielectric strength. In *Polymer Science Dictionary*, ed. M. Alger, pp 137–139. United Kingdom: Chapman & Hall.
- Avdeev, M., Haas, M.K., Jorgensen, J.D. and Cava, R.J. 2002. Static disorder from lone-pair electrons in  $\text{Bi}_{2-x}\text{M}_x\text{Ru}_2\text{O}_{7-y}$  (M = Cu, Co; x = 0, 0.4) pyrochlores. *Journal of Solid State Chemistry* 169(1): 24–34.
- Bagshaw, A.N. 1976. Diverse structures based on the Fd3m space group. *Journal of Crystallography-Crystalline Materials* 144(1–6): 53–63.
- Bard, A.J., Inzelt, G. and Scholz, F. 2012. Impedance. In *Impedance Dictionary*, ed. A. Bard, G. Inzelt and F. Scholz, pp 479–481. New York: Springer Heidelberg Dordrecht.
- Barsoum, M.W. 2003. Introduction. In *Fundamentals of Ceramics*, ed. M.W. Barsoum, pp 1–11. New York: Taylor & Francis Group.
- Bartnikas, R. 1987. Direct current conductivity measurements. In *Engineering Dielectrics Volume IIB: Electrical Properties of Solid Insulating Materials: Measurement Techniques*, ed. R. Bartnikas, pp 3–10. Canada: America Society for Testing and Materials.
- Beck, E., Ehmann, A., Krutzsch, B., Kemmler-Sack, S., Khan, H.R. and Raub, C.J. 1989. Investigation of superconductivity and physical properties of some spinel-, perovskite- and pyrochlore-type oxides. *Journal of the Less Common Metals* 147(2): L17–L20.
- Beguín, F. and Frąckowiak, E. 2010. In *Carbons for Electrochemical Energy Storage and Conversion Systems*. CRC Press.
- Boikov, Y.A. and Claeson, T. 1997. High tunability of the permittivity of  $\text{YBa}_2\text{Cu}_3\text{O}_{7-x}/\text{SrTiO}_3$  heterostructures on sapphire substrates. *Journal of Applied Physics* 81(7): 3232–3236.
- Brise, F., Stewart, D.J., Seidl, V. and Knop, O. 1972. Pyrochlores. VIII. Studies of some 2-5 pyrochlores and related compounds and minerals. *Canadian Journal of Chemistry* 50(22): 3648–3666.
- Brown, M.E. 1988. Thermal gravimetry (TG), differential thermal analysis (DTA) and differential scanning calorimetry (DSC). In *Introduction to Thermal Analysis: Techniques and Applications*, ed. M.E. Brown, pp 19–21 and 23–49. London: Chapman & Hall, Ltd.

- Cann, D.P., Randall, C.A. and Shrout, T.R. 1996. Investigation of the dielectric properties of bismuth pyrochlores. *Solid State Communications* 100(7): 529–534.
- Chang, S.K., 2012. Structural and electrochemical properties of nickel-cobalt oxide/activated carbon for supercapacitor application, Ph.D Thesis, Universiti Putra Malaysia.
- Chang, S.K., Lee, K.T., Zainal, Z., Tan, K.B., Yusof, N.A., Yusoff, W.M.D.W., Lee, J.F. and Wu, N.L. 2012a. Structural and electrochemical properties of manganese substituted nickel cobaltite for supercapacitor application. *Electrochimica Acta* 67: 67–72.
- Chang, S.K., Zainal, Z., Tan, K.B., Yusof, N.A., Yusoff, W.M.D.W. and Prabaharan, S.R.S. 2012b. Nickel-cobalt oxide/activated carbon composite electrodes for electrochemical capacitors. *Current Applied Physics* 12(6): 1421–1428.
- Chaudhari, V.A. and Bichile, G.K. 2013. Synthesis, structural, and electrical properties of pure  $\text{PbTiO}_3$  ferroelectric ceramics. *Smart Materials Research* 2013.
- Chee, W.K., Lim, H.N. and Huang, N.M. 2015. Electrochemical properties of free-standing polypyrrole/graphene oxide/zinc oxide flexible supercapacitor. *International Journal of Energy Research* 39(1): 111–119.
- Chen, M., Tanner, D.B. and Nino, J.C. 2005. Infrared study of the phonon modes in bismuth pyrochlores. *Physical Review B* 72(5): 054303.
- Chen, S.Y., Lee, S.Y. and Lin, Y.J. 2003. Phase transformation, reaction kinetics and microwave characteristics of  $\text{Bi}_2\text{O}_3\text{-ZnO-Nb}_2\text{O}_5$  ceramics. *Journal of the European Ceramic Society* 23(6): 873–881.
- Cheng, H.F., Chen, Y.C. and Lin, I.N. 2000. Frequency response of microwave dielectric  $\text{Bi}_2(\text{Zn}_{1/3}\text{Nb}_{2/3})_2\text{O}_7$  thin films laser deposited on indium-tin oxide coated glass. *Journal of Applied Physics* 87(1): 479–483.
- Chon, M.P., Tan, K.B., Khaw, C.C., Zainal, Z., Taufiq-Yap, Y.H., Chen, S.K. and Tan, P.Y. 2016a. Subsolidus phase equilibria and electrical properties of pyrochlores in the  $\text{Bi}_2\text{O}_3\text{-CuO-Ta}_2\text{O}_5$  ternary system. *Journal of Alloys and Compounds* 675: 116–127.
- Chon, M.P., Tan, K.B., Zainal, Z., Taufiq-Yap, Y.H., Tan, P.Y., Khaw, C.C. and Chen, S.K. 2016b. Synthesis and electrical properties of Zn-substituted bismuth copper tantalate pyrochlores. *International Journal of Applied Ceramic Technology* 13(4): 718–725.
- Christou, A. 2006. Manufacturing of electronic microwave substrates for packaging of monolithic microwave circuits. In *Reliability and Quality in Microelectronic Manufacturing*, ed. A. Christou, pp 341–350. United States of America.

- Cole, K.S. and Cole, R.H. 1941. Dispersion and absorption in dielectrics I. Alternating current characteristics. *The Journal of Chemical Physics* 9(4): 341–351.
- Conway, B.E. 1999. In *Electrochemical Supercapacitors: Scientific, Fundamentals and Technological Applications*. New York: Plenum.
- Darriet, B., Rat, M., Galy, J. and Hagenmuller, P. 1971. On some new pyrochlores of systems of  $\text{MTO}_3\text{-WO}_3$  and  $\text{MTO}_3\text{-TeO}_3$  ( $\text{M} = \text{K, Rb, Cs, Tl}$ ;  $\text{T} = \text{Nb, Ta}$ ). *Materials Research Bulletin* 6(12): 1305–1315.
- Dasin, N.A.M., Tan, K.B., Khaw, C.C., Zainal, Z. and Chen, S.K. 2017. Subsolidus solution and electrical properties of Sr-substituted bismuth magnesium niobate pyrochlores. *Ceramics International* 43(13): 10183–10191.
- Du, H. and Yao, X. 2001. Investigation of dielectric properties of  $\text{Bi}_2\text{O}_3\text{-ZnO-Nb}_2\text{O}_5\text{-Sb}_2\text{O}_3$  based pyrochlores. *Ferroelectrics* 262(1): 83–88.
- Du, H. and Yao, X. 2003. Effects of Sr substitution on dielectric characteristics in  $\text{Bi}_{1.5}\text{ZnNb}_{1.5}\text{O}_7$  ceramics. *Materials Science and Engineering: B* 99(1): 437–440.
- Du, H. and Yao, X. 2004. Structural trends and dielectric properties of Bi-based pyrochlores. *Journal of Materials Science: Materials in Electronics* 15(9): 613–616.
- Du, H., Yao, X. and Wang, H. 2001. The effect of CuO on sintering and dielectric properties of  $\text{Bi}_2\text{O}_3\text{-ZnO-Nb}_2\text{O}_5$  pyrochlore. *Ferroelectrics* 262(1): 89–94.
- Du, H., Yao, X. and Zhang, L. 2002. Structure, IR spectra and dielectric properties of  $\text{Bi}_2\text{O}_3\text{-ZnO-SnO}_2\text{-Nb}_2\text{O}_5$  quarternary pyrochlore. *Ceramics International* 28(3): 231–234.
- Eskola, P. 1922. The silicates of strontium and barium. *American Journal of Science* 23: 331–375.
- Findikoglu, A.T., Jia, Q.X. and Reagor, D.W. 1997. Superconductor/nonlinear-dielectric bilayers for tunable and adaptive microwave devices. *IEEE Transactions on Applied Superconductivity* 7(2): 2925–2928.
- Fiore, R. 2000. *Circuit designer's notebook*. American Technical Ceramics.
- Gaines, R.V., Skinner, H.C.W., Foord, E.E. and Rosenzweig, A. 1997. *Dana's New Mineralogy*, ed. R.V. Gaines, H.C.W. Skinner, E.E. Foord and A. Rosenzweig, pp 341–352. New York: Wiley.
- Gao, L., Jiang, S., Li, R., Li, B. and Li, Y. 2013. Influence of post deposition annealing on crystallinity and dielectric properties of bismuth magnesium niobate thin films. *Applied Surface Science* 284: 523–526.

- Gao, L., Jiang, S., Li, R., Li, B. and Li, Y. 2014. Effect of magnesium content on structure and dielectric properties of cubic bismuth magnesium niobate pyrochlores. *Ceramics International* 40(3): 4225–4229.
- Garrison, E.G. 2003. X-ray diffraction. In *Techniques in Archaeological Geology*, ed. E.G. Garrison, pp 212. New York: Springer-Verlag Berlin Heidelberg.
- Gevorgian, S., Carlsson, E., Linner, P., Kollberg, E., Vendik, O. and Wikborg, E. 1996. Lower order modes of YBCO/STO/YBCO circular disk resonators. *IEEE Transactions on Microwave Theory and Techniques* 44(10): 1738–1741.
- Gnanaswara-Rao, K.V.S. 2008. Orientation polarisation. In *Engineering Physics*, ed. K.V.S. Gnanaswara Rao, pp 82. New Delhi: S. Chand & Company LTD.
- Goldman, A. 2006. Basics of magnetism. In *Modern Ferrite Technology*, ed. A. Goldman, pp 1–14. New York: Springer Science + Business Media, Inc.
- Golonka, L.J. 2006. Technology and applications of low temperature cofired ceramic (LTCC) based sensors and microsystems. *Bulletin of the Polish Academy of Sciences Technical Sciences* 54(2).
- Hector, A.L. and Wiggin, S.B. 2004. Synthesis and structural study of stoichiometric  $\text{Bi}_2\text{Ti}_2\text{O}_7$  pyrochlore. *Journal of Solid State Chemistry* 177(1): 139–145.
- Heywang, W. and Thomann, H. 1991. Positive temperature coefficient resistors. *Electronic Ceramics* 29–48.
- Higgins, T.M., McAteer, D., Coelho, J.C.M., Sanchez, B.M., Gholamvand, Z., Moriarty, G., McEvoy, N., Berner, N.C., Duesberg, G.S., Nicolosi, V. and Coleman, J.N. 2014. Effect of percolation on the capacitance of supercapacitor electrodes prepared from composites of manganese dioxide nanoplatelets and carbon nanotubes. *Acs Nano* 8(9): 9567–9579.
- Ho, P.S., Lee, W.W. and Leu, J. 2002. Low dielectric constant materials for IC applications. *Journal Research Development* 50 (4/5): 387.
- Hoerman, B.H., Ford, G.M., Kaufmann, L.D. and Wessels, B.W. 1998. Dielectric properties of epitaxial  $\text{BaTiO}_3$  thin films. *Applied Physics Letters* 73(16): 2248–2250.
- Illig, J. 2014. Electrochemical impedance spectroscopy. In *Physically Based Impedance Modelling of Lithium-ion Cells*, ed. J. Illig, pp 24–25. Karlsruhe Institut for Technology (KIT).
- Irvine, J.T.S., Sinclair, D.C. and West, A.R. 1990. Electroceramics: characterisation by impedance spectroscopy. *Advance Materials* 2: 132–138.
- Ismunandar, B.J.K. and Hunter, B.A. 1998. Temperature dependent neutron powder diffraction study of  $\text{Bi}_3(\text{GaSb}_2)\text{O}_{11}$ . *Solid State Communications* 108(9): 649–654.

- Jack, C.B. and George, W.T. 1979. Polar dielectrics and their applications. *Physics Bulletin* 31(5): 176.
- Jang, J.H., Han, S., Hyeon, T., and Oh, S.M. 2003. Electrochemical capacitor performance of hydrous ruthenium oxide/mesoporous carbon composite electrodes. *Journal of power sources* 123(1): 79–85.
- Jiang, S.W., Li, Y.R., Li, R.G., Xiong, N.D., Tan, L.F., Liu, X.Z. and Tao, B.W. 2009. Dielectric properties and tunability of cubic pyrochlore  $\text{Bi}_{1.5}\text{MgNb}_{1.5}\text{O}_7$  thin films. *Applied Physics Letters* 94(16): 162908.
- Jones, W. and Thomas, J.M. 1979. Applications of electron microscopy to organic solid state chemistry. *Progress in Solid State Chemistry* 12: 101–124.
- Jonscher, A.K. 1999. Dielectric relaxation in solids. *Journal of Physics D: Applied Physics* 32(14): R57.
- Justin, P., Meher, S.K. and Rao, G.R. 2010. Tuning of capacitance behavior of NiO using anionic, cationic, and nonionic surfactants by hydrothermal synthesis. *The Journal of Physical Chemistry C* 114(11): 5203–5210.
- Kamba, S., Bovtun, V., Petzelt, J., Rychetsky, I., Mizaras, R., Brilingas, A., Banys, J., Grigas, J. and Kosec, M. 2000. Dielectric dispersion of the relaxor PLZT ceramics in the frequency range 20 Hz–100 THz. *Journal of Physics: Condensed Matter* 12(4): 497.
- Kamba, S., Porokhonsky, V., Pashkin, A., Bovtun, V., Petzelt, J., Nino, J.C., Trolier-McKinstry, S., Lanagan, M.T. and Randall, C.A. 2002. Anomalous broad dielectric relaxation in  $\text{Bi}_{1.5}\text{Zn}_{1.0}\text{Nb}_{1.5}\text{O}_7$  pyrochlore. *Physical Review B* 66(5): 054106.
- Kannappan, S., Kaliyappan, K., Manian, R.K., Pandian, A.S., Yang, H., Lee, Y.S., Jang, J.H. and Lu, W. 2013. Graphene based supercapacitors with improved specific capacitance and fast charging time at high current density. *arXiv preprint arXiv* 1311.1548.
- Karanovic, L., Poleti, D., and Vasovic, D. 1994. On the possibility of pyrochlore phase formation in zinc oxide varistor ceramic. *Materials Letters* 18(4): 191–196.
- Kennedy, B.J. 1997. Structural trends in pyrochlore-type oxides. *Physica B: Condensed Matter* 241: 303–310.
- Khaw, C.C., Tan, K.B. and Lee, C.K. 2009. High temperature dielectric properties of cubic bismuth zinc tantalate. *Ceramics International* 35(4): 1473–1480.
- Khaw, C.C., Tan, K.B., Lee, C.K. and West, A.R. 2012. Phase equilibria and electrical properties of pyrochlore and zirconolite phases in the  $\text{Bi}_2\text{O}_3$ -ZnO-Ta<sub>2</sub>O<sub>5</sub> system. *Journal of the European Ceramic Society* 32(3): 671–680.



- Kim, K.J. and Tadokoro, S. 2007. Polarisability and polarisation. In *Electroactive Polymers for Robotic Applications: Artificial Muscles and Sensors*, ed. K.J. Kim and S. Tadokoro, pp 93–95. USA.
- Kim, S.S., and Kim, W.J. 2005. Electrical properties of sol-gel derived pyrochlore-type bismuth magnesium niobate  $\text{Bi}_2(\text{Mg}_{1/3}\text{Nb}_{2/3})_2\text{O}_7$  thin films. *Journal of Crystal Growth* 281(2): 432–439.
- Koizumi, H., Noma, A., Tanaka, R., Kanazawa, K., and Ueda, D. 1996. A GaAs MMIC chip-set for mobile communications using on-chip ferroelectric capacitors. *IEEE Journal of Solid-State Circuits* 31(6): 835–840.
- Kong, L.B., Huang, Y.Z., Que, W.X., Zhang, T.S., Li, S., Zhang, J., Dong, Z.L., and Tang, D.Y. 2015. Transparent ceramic materials. In *Transparent Ceramics*, ed. L.B. Kong, Y.Z. Huang, W.X. Que, T.S. Zhang, S. Li, J. Zhang, Z.L. Dong and D.Y. Tang, pp 29–77. New York: Springer Chan Heidelberg.
- Kwan, C.K. 2004. Electrical transport by a hopping process. In *Dielectric Phenomena in Solids: With Emphasis on Physical Concepts of Electronic Processes*, ed. C.K. Kwan, pp 401. United Kingdom: Elsevier Academic Press.
- La Tour, T.E. 1989. Analysis of rocks using X-ray fluorescence spectrometry. *The Rigaku Journal* 6(1): 3–9.
- Lambachri, A., Manier, M., Mercurio, J.P. and Frit, B. 1988. New dielectric ceramics  $\text{Pb}(\text{Cd})\text{BiM}^{\text{IV}}\text{SbO}_7$  ( $\text{M}^{\text{IV}} = \text{Ti}, \text{Zr}, \text{Sn}$ ) with the pyrochlore structure. *Materials Research Bulletin* 23(4): 571–578.
- Lee, H.Y., and Goodenough, J.B. 1999. Supercapacitor behavior with KCl electrolyte. *Journal of Solid State Chemistry* 144(1): 220–223.
- Levin, I., Amos, T.G., Nino, J.C., Vanderah, T.A., Randall, C.A. and Lanagan, M.T. 2002a. Structural study of an unusual cubic pyrochlore  $\text{Bi}_{1.5}\text{Zn}_{0.92}\text{Nb}_{1.5}\text{O}_{6.92}$ . *Journal of Solid State Chemistry* 168(1): 69–75.
- Levin, I., Amos, T.G., Nino, J.C., Vanderah, T.A., Reaney, I.M., Randall, C.A. and Lanagan, M.T. 2002b. Crystal structure of the compound  $\text{Bi}_2\text{Zn}_{2/3}\text{Nb}_{4/3}\text{O}_7$ . *Journal of Materials Research* 17(6): 1406–1411.
- Li, H.C., Si, W., West, A.D. and Xi, X.X. 1998. Near single crystal-level dielectric loss and nonlinearity in pulsed laser deposited  $\text{SrTiO}_3$  thin films. *Applied Physics Letters* 73(2): 190–192.
- Li, L. and Kennedy, B.J. 2003. Structural and electronic properties of the Ru pyrochlores  $\text{Bi}_{2-y}\text{Yb}_y\text{Ru}_2\text{O}_{7-\delta}$ . *Chemistry of Materials* 15(21): 4060–4067.
- Li, L., Xu, D., Yu, S., Dong, H., Jin, Y. and Zheng, H. 2014a. Effect of substrate on the dielectric properties of bismuth magnesium niobate thin films prepared by RF magnetron sputtering. *Vacuum* 109: 21–25.

- Li, L., Zhang, X., Ji, L., Ning, P. and Liao, Q. 2012. Dielectric properties and electrical behaviors of tunable  $\text{Bi}_{1.5}\text{MgNb}_{1.5}\text{O}_7$  thin films. *Ceramics International* 38(5): 3541–3545.
- Li, Y., Zhu, X. and Kassab, T.A. 2014b. Atomic-scale microstructures, Raman spectra and dielectric properties of cubic pyrochlore-typed  $\text{Bi}_{1.5}\text{MgNb}_{1.5}\text{O}_7$  dielectric ceramics. *Ceramics International* 40(6): 8125–8134.
- Liu, D., Liu, Y., Huang, S.Q. and Yao, X. 1993. Phase structure and dielectric properties of  $\text{Bi}_2\text{O}_3$ - $\text{ZnO}$ - $\text{Nb}_2\text{O}_5$ -Based dielectric ceramics. *Journal of the American Ceramic Society* 76(8): 2129–2132.
- Lu, J. and Stemmer, S. 2003. Low-loss, tunable bismuth zinc niobate films deposited by rf magnetron sputtering. *Applied Physics Letters* 83(12): 2411–2413.
- Macdonald, J.R. 1953. Theory of ac space-charge polarization effects in photoconductors, semiconductors, and electrolytes. *Physical Review* 92(1): 4.
- Macdonald, J.R. and Johnson, W.B. 2005. Fundamentals of impedance spectroscopy. In *Impedance Spectroscopy-Theory, Experiment, and Applications*, ed. J.R. Macdonald and W.B. Johnson, pp 1–26. New Jersey: Wiley-Interscience.
- Maheshwari, P. 2006. Ionic polarisation (molecular polarisation). In *Electronic Components and Processes*, ed. P. Maheshwari, pp 59–61. New Delhi: New Age International (P) Limited.
- Marikani, A. 2017. Ionic polarisation. In *Materials Science*, ed. A. Marikani, pp 290–293. New Delhi: PHI Learning Private Limited.
- Martin, S.W., Yao, W. and Berg, K. 2009. Space charge polarization measurements as a method to determine the temperature dependence of the number density of mobile cations in ion conducting glasses. *International Journal of Research in Physical Chemistry and Chemical Physics* 223(10–11): 1379–1393.
- Mayer-Von Kuerthy, G., Wischert, W., Kiemel, R., Kemmler-Sack, S., Gross, R. and Huebener, R.P. 1989. System  $\text{Bi}_{2-x}\text{Pb}_x\text{Pt}_{2-x}\text{Ru}_x\text{O}_{7-z}$ : A pyrochlore series with a metal-insulator transition. *Journal of Solid State Chemistry* 79(1): 34–45.
- Mergen, A. and Lee, W.E. 1997. Crystal chemistry, thermal expansion and dielectric properties of  $(\text{Bi}_{1.5}\text{Zn}_{0.5})(\text{Sb}_{1.5}\text{Zn}_{0.5})\text{O}_7$  pyrochlore. *Materials Research Bulletin* 32(2): 175–189.
- Mitchell, B.S. 2004. Electrical properties of ceramics and glasses. In *An Introduction to Materials Engineering and Science: For Chemical and Materials Engineers*, ed. B.S. Mitchell, pp 561–575. New York: John Wiley & Sons, Ltd.
- Moulson, A.J. and Herbert, J.M. 2003. Ceramic conductors. In *Electroceraamics: Materials, Properties, Applications*, ed. A.J. Moulson and J.M. Herbert, pp 135–242. New York: John Wiley & Sons, Ltd.



- Mueller, C.H., Miranda, F.A., Toncich, S.S. and Bhasin, K.B. 1995. YBCO X-band microstrip linear resonators on (1. *IEEE Transactions on Applied Superconductivity* 5(2): 2559–2562.
- Muktha, B., Darriet, J., Madras, G. and Row, T.G. 2006. Crystal structures and photocatalysis of the triclinic polymorphs of BiNbO<sub>4</sub> and BiTaO<sub>4</sub>. *Journal of Solid State Chemistry* 179(12): 3919–3925.
- Murarka, S.P., Eizenbergh, M. And Sinha, A.K. 2003. Interlayer dielectrics for semiconductor technologies. *Elsevier/Academic press, Amsterdam, Boston* 12–14: 194.
- Nalwa, H.S. 1999. Materials requirements: Dielectric constant. *Handbook of Low and High Dielectric Constant Materials and their Applications* 495.
- Nanni, P., Viviani, M. and Buscaglia, V. 1999. Synthesis of dielectric ceramic materials. *Handbook of Low and High Dielectric Constant Materials and their Applications* 1:429–455.
- Nenasheva, E.A. and Kartenko, N.F. 2006. Low-sintering ceramic materials based on Bi<sub>2</sub>O<sub>3</sub>-ZnO-Nb<sub>2</sub>O<sub>5</sub> compounds. *Journal of the European Ceramic Society* 26(10): 1929–1932.
- Nguyen, B., Yun, L. and Withers, R.L. 2007. The local crystal chemistry and dielectric properties of the cubic pyrochlore phase in the Bi<sub>2</sub>O<sub>3</sub>-M<sup>2+</sup>O-Nb<sub>2</sub>O<sub>5</sub> (M<sup>2+</sup> = Ni<sup>2+</sup> and Mg<sup>2+</sup>) systems. *Journal of Solid State Chemistry* 180(2): 549–557.
- Nino, J.C., Lanagan, M.T. and Randall, C.A. 2001. Dielectric relaxation in Bi<sub>2</sub>O<sub>3</sub>-ZnO-Nb<sub>2</sub>O<sub>5</sub> cubic pyrochlore. *Journal of Applied Physics* 89(8): 4512–4516.
- Nino, J.C., Youn, H.J., Lanagan, M.T. and Randall, C.A. 2002. Bi<sub>2</sub>O<sub>3</sub> solubility of Bi-based pyrochlores and related phases. *Journal of Materials Research* 17(5): 1178–1182.
- Nobre, M.A.L. and Lanfredi, S. 2001. Dielectric properties of Bi<sub>3</sub>Zn<sub>2</sub>Sb<sub>3</sub>O<sub>14</sub> ceramics at high temperature. *Materials Letters* 47(6): 362–366.
- Nobre, M.A.L. and Lanfredi, S. 2002. The effect of temperature on the electric conductivity property of Bi<sub>3</sub>Zn<sub>2</sub>Sb<sub>3</sub>O<sub>14</sub> pyrochlore type phase. *Journal of Materials Science: Materials in Electronics* 13(4): 235–238.
- Nobre, M.A.L., and Lanfredi, S. 2003. Dielectric spectroscopy on Bi<sub>3</sub>Zn<sub>2</sub>Sb<sub>3</sub>O<sub>14</sub> ceramic: an approach based on the complex impedance. *Journal of Physics and Chemistry of Solids*, 64(12), 2457-2464.
- Nyquist, R.A. and Kagel, R.O. 1971. Infrared spectra of inorganic compounds- Introduction. In *Infrared spectra of inorganic compounds*, ed. R.A. Nyquist and R.O. Kagel, pp 1–4. New York: Academic press, Inc.

- Orazem, M.E. and Tribollet, B. 2008. History of impedance spectroscopy. In *Electrochemical Impedance Spectroscopy (EIS)*, ed. M.E. Orazem and B. Tribollet, pp 5–10. New York: John Wiley & Sons, Ltd.
- Petrov, P.K., Carlsson, E.F., Larsson, P., Friesel, M. and Ivanov, Z.G. 1998. Improved SrTiO<sub>3</sub> multilayers for microwave application: Growth and properties. *Journal of Applied Physics* 84(6): 3134–3140.
- Prasad, N.V., Sekhar, M.C. and Kumar, G.S. 2008. Impedance spectroscopic studies on lead based perovskite materials. *Ferroelectrics* 366(1): 55–66.
- Raju, G.G. 2009. Polarisation and static dielectric constant. In *Dielectrics in Electric Fields*, ed. G.G. Raju, pp 35–49. New York: Taylor & Francis e-Library.
- Rao, P.P., Liji, S.J., Nair, K.R. and Koshy, P. 2004. New pyrochlore-type oxides in Ca-R-Ti-Nb-O system (R = Y, Sm or Gd)-structure, FT-IR spectra and dielectric properties. *Materials Letters* 58(12): 1924–1927.
- Ray, F.E. 2005. The scanning electron microscopy (SEM). In *Physical Principles of Electron Microscopy: An Introduction to TEM, SEM and AEM*, ed. F.E. Ray, pp 125–143. Canada: University of Alberta.
- Reid, A.F., Li, C. and Ringwood, A.E. 1977. High-pressure silicate pyrochlores, Sc<sub>2</sub>Si<sub>2</sub>O<sub>7</sub> and In<sub>2</sub>Si<sub>2</sub>O<sub>7</sub>. *Journal of Solid State Chemistry* 20(3): 219–226.
- Ren, W., Trolier-McKinstry, S., Randall, C.A. and Shrout, T.R. 2001. Bismuth zinc niobate pyrochlore dielectric thin films for capacitive applications. *Journal of Applied Physics* 89(1): 767–774.
- Riedel, R. and Chen, I-W. 2014. Magnetic ceramics. In *Ceramics Science and Technology, Applications*, ed. R. Riedel and I-W. Chen, pp 14–24. Germany: Wiley-VCH Verlag GmbH & Co.
- Ronchi, C. and Sheindlin, M. 2001. Melting point of MgO. *Journal of Applied Physics* 90(7): 3325–3331.
- Sawada, A., Tarumi, K. and Naemura, S. 1999. Effects of electric double layer and space charge polarization by plural kinds of ions on complex dielectric constant of liquid crystal materials. *Japanese Journal of Applied Physics* 38(3R): 1418.
- Sebastian, M.T. 2008. Measurement of microwave dielectric properties and factors affecting them. In *Dielectric Materials for Wireless Communication*, ed. M.T. Sebastian, pp 33–37. Jordan Hill: Oxford.
- Setter, N. and Waser, R. 2000. Electroceramic materials. *Acta Materialia* 48(1): 151–178.
- Shannon, R.D. 1976. Revised effective ionic radii and systematic studies of interatomic distances in halides and chalcogenides. *Acta crystallographica section A*:

*crystal physics, diffraction, theoretical and general crystallography* 32(5): 751–767.

- Shannon, R.D. 1993. Dielectric polarizabilities of ions in oxides and fluorides. *Journal of Applied Physics* 73(1): 348–366.
- Shannon, R.D. and Sleight, A.W. 1968. Synthesis of new high-pressure pyrochlore phases. *Inorganic Chemistry* 7(8): 1649–1651.
- Sinclair, D.C., Morrison, F.D. and West, A.R. 2000. Applications of combined impedance and electric modulus spectroscopy to characterise electroceramics. *International Ceramics* 2: 33–34.
- Sirotkin, V.P. and Bush, A.A. 2003. Preparation and dielectric properties of  $\text{Bi}_{1.5}\text{MNb}_{1.5}\text{O}_7$  (M = Cu, Mg, Mn, Ni, Zn) pyrochlore oxides. *Inorganic Materials* 39(9): 974–977.
- Skoog, D.A., Holler, F.J. and Nieman, T.A. 1997. Inductively coupled plasma-optical emission spectroscopy (ICP-OES). In *Principles of Instrumental Analysis*, ed. 5<sup>th</sup>, pp 10–15. Harcourt College Publishers.
- Subramanian, M.A., Aravamudan, G. and Rao, G.S. 1983. Oxide pyrochlores-a review. *Progress in Solid State Chemistry* 15(2): 55–143.
- Syed, M., Prasad, G. and Kumar, G.S. 2006. Study of dielectric and impedance relaxations in  $(\text{Na}_{0.125}\text{Bi}_{0.125}\text{Ba}_{0.65}\text{Ca}_{0.1})(\text{Nd}_{0.065}\text{Ti}_{0.87}\text{Nb}_{0.065})\text{O}_3$  ceramic. *Materials Chemistry and Physics* 99(2): 276–283.
- Tan, K.B., Chon, M.P., Khaw, C.C., Zainal, Z., Taufiq-Yap, Y.H., Chen, S.K. and Tan, P.Y. 2017. Phase equilibria in the  $\text{Bi}_2\text{O}_3$ -CuO-Nb<sub>2</sub>O<sub>5</sub> ternary system. *Ceramics International* 43(6): 4930–4936.
- Tan, K.B., Khaw, C.C., Lee, C.K., Zainal, Z. and Miles, G.C. 2010. Structures and solid solution mechanisms of pyrochlore phases in the systems  $\text{Bi}_2\text{O}_3$ -ZnO-(Nb, Ta)<sub>2</sub>O<sub>5</sub>. *Journal of Alloys and Compounds* 508(2): 457–462.
- Tan, K.B., Khaw, C.C., Lee, C.K., Zainal, Z., Tan, Y.P. and Shaari, H. 2009. High temperature impedance spectroscopy study of non-stoichiometric bismuth zinc niobate pyrochlore. *Materials Science-Poland* 27(3): 825–837.
- Tan, K.B., Lee, C.K., Zainal, Z., Khaw, C.C., Tan, Y.P. and Shaari, H. 2008. Reaction study and phase formation in  $\text{Bi}_2\text{O}_3$ -ZnO-Nb<sub>2</sub>O<sub>5</sub> ternary system. *Pacific Journal of Science and Technology* 9(2): 468–79.
- Tan, K.B., Lee, C.K., Zainal, Z., Miles, G.C. and West, A.R. 2005. Stoichiometry and doping mechanism of the cubic pyrochlore phase in the system  $\text{Bi}_2\text{O}_3$ -ZnO-Nb<sub>2</sub>O<sub>5</sub>. *Journal of Materials Chemistry* 15(34): 3501–3506.
- Tan, K.B., Lee, C.K., Zainal, Z., Tan, Y.P. and Shaari, A.H. 2007. Phase study and electrical properties of divalent doped non-stoichiometric bismuth zinc

niobate cubic pyrochlore. *Journal of Solid State Science and Technology* 15(1): 74–81.

- Tan, P.Y., 2015. Preparation and characterisation of dielectric pyrochlores in the  $\text{Bi}_2\text{O}_3\text{-MgO-M}_2\text{O}_5$  ( $\text{M} = \text{Ta}$  and  $\text{Nb}$ ) ternary systems, Ph.D Thesis, Universiti Putra Malaysia.
- Tan, P.Y., Tan, K.B., Khaw, C.C., Zainal, Z. and Chen, S.K. 2011. Synthesis and characterization of  $\text{Bi}_3\text{Mg}_2\text{Nb}_3\text{O}_{14}$  pyrochlore system. *Solid State Science and Technology* 19(2): 221–231.
- Tan, P.Y., Tan, K.B., Khaw, C.C., Zainal, Z., Chen, S.K. and Chon, M.P. 2014. Phase equilibria and dielectric properties of  $\text{Bi}_{3+(5/2)x}\text{Mg}_{2-x}\text{Nb}_{3-(3/2)x}\text{O}_{14-x}$  cubic pyrochlores. *Ceramics International* 40(3): 4237–4246.
- Tan, P.Y., Tan, K.B., Khaw, C.C., Zainal, Z., Chen, S.K. and Chon, M.P. 2012. Structural and electrical properties of bismuth magnesium tantalate pyrochlores. *Ceramics International* 38(7): 5401–5409.
- Thayer, R.L., Randall, C.A. and Trolrier-McKinstry, S. 2003. Medium permittivity bismuth zinc niobate thin film capacitors. *Journal of Applied Physics* 94(3): 1941–1947.
- Valant, M. and Davies, P.K. 2000. Crystal chemistry and dielectric properties of chemically substituted  $(\text{Bi}_{1.5}\text{Zn}_{1.0}\text{Nb}_{1.5})\text{O}_7$  and  $\text{Bi}_2(\text{Zn}_{2/3}\text{Nb}_{4/3})\text{O}_7$  pyrochlores. *Journal of the American Ceramic Society* 83(1): 147–53.
- Vanderah, T.A., Levin, I. and Lufaso, M.W. 2005. An Unexpected crystal-chemical principle for the pyrochlore structure. *European Journal of Inorganic Chemistry* 2005(14): 2895–2901.
- Vendik, O.G., Kollberg, E., Gevorgian, S.S., Kozyrev, A.B. and Soldatenkov, O.I. 1995. 1 GHz tunable resonator on bulk single crystal  $\text{SrTiO}_3$ /sub 3/plated with  $\text{YBa}/\text{sub } 2/\text{Cu}/\text{sub } 3/\text{O}/\text{sub } 7-x$ /films. *Electronics Letters* 31(8): 654–656.
- Wang, C.C., Linke, R.A., Nolte, D.D., Melloch, M.R. and Trivedi, S. 1998. Signal strength enhancement and bandwidth tuning in moving space charge field photodetectors using alternating bias field. *Applied Physics Letters* 72(1): 100–102.
- Wang, H., Du, H., Peng, Z., Zhang, M. and Yao, X. 2004. Improvements of sintering and dielectric properties on  $\text{Bi}_2\text{O}_3\text{-ZnO-Nb}_2\text{O}_5$  pyrochlore ceramics by  $\text{V}_2\text{O}_5$  substitution. *Ceramics International* 30(7): 1225–1229.
- Wang, H., Zhang, D., Wang, X. and Yao, X. 1999. Effect of  $\text{La}_2\text{O}_3$  substitutions on structure and dielectric properties of  $\text{Bi}_2\text{O}_3\text{-ZnO-Nb}_2\text{O}_5$ -based pyrochlore ceramics. *Journal of Materials Research* 14(2): 546–548.

- Wang, X., Wang, H. and Yao, X. 1997. Structures, phase transformations, and dielectric properties of pyrochlores containing bismuth. *Journal of the American Ceramic Society* 80(10): 2745–2748.
- Wen, L.C., Hsieh, H.Y., Lee, Y.H., Chang, S.C., Kao, H.C.I., Sheu, H.S., Lin, I.N., Chang, J.C., Lee, M.C. and Lee, Y.S. 2012. Preparation of compact Li-doped  $\text{Y}_2\text{Ti}_2\text{O}_7$  solid electrolyte. *Solid State Ionics* 206: 39–44.
- West, A.R. 1999a. Crystallography and diffraction techniques. In *Basic Solid State Chemistry*, ed. A.R. West, pp 125–135. New York: John Wiley & Sons, Ltd.
- West, A.R. 1999b. Differential thermal analysis (DTA) and differential scanning calorimetry (DSC). In *Basic Solid State Chemistry*, ed. A.R. West, pp 204–206. New York: John Wiley & Sons, Ltd.
- West, A.R. 1999c. X-ray spectroscopies: XRF, AEFS, EXAFS. In *Basic Solid State Chemistry*, ed. A.R. West, pp 189–191. New York: John Wiley & Sons, Ltd.
- Williamson, G.K. and Hall, W.H. 1953. X-ray line broadening from fcc aluminium and wolfram. *Acta Metallurgica* 1(1): 22–31.
- Withers, R.L., Welberry, T.R., Larsson, A.K., Liu, Y., Noren, L., Rundlof, H. and Brink, F.J. 2004. Local crystal chemistry, induced strain and short range order in the cubic pyrochlore  $(\text{Bi}_{1.5-\alpha}\text{Zn}_{0.5-\beta})(\text{Zn}_{0.5-\gamma}\text{Nb}_{1.5-\delta})\text{O}_{(7-1.5\alpha-\beta-\gamma-2.5\delta)}$ (BZN). *Journal of Solid State Chemistry* 177(1): 231–244.
- Xian, C.J., Park, J.H., Ahn, K.C., Yoon, S.G., Lee, J.W., Kim, W.C., Lim, S.T., Sohn, S.H., Moon, J.S., Jung, H.M., Lee, S.E., Lee, I.H., Chung, Y.K., Jeon, M.K. and Woo, S.I. 2007a. Electrical properties of  $\text{Bi}_2\text{Mg}_2\text{Nb}_4\text{O}_7$  (BMN) pyrochlore thin films deposited on Pt and Cu metal at low temperatures for embedded capacitor applications. *Applied Physics Letters* 90(5): 052903.
- Xian, C.J., Park, J.H., Yoon, S.G., Moon, J.S., Lim, S.T., Sohn, S.H., Jung, H.M., Shin, Y.N., Woon, C.K., Jeon, M.K. and Woo, S.I. 2007b. Effect of thickness on electrical properties of bismuth-magnesium niobate pyrochlore thin films deposited at low temperature. *Journal of Applied Physics* 101(8): 084114.
- Yanping, L., Xi, Y., Bo, S. and Liangying, Z. 2001a. Synthesis, structure and dielectric properties of  $\text{Bi}_2\text{O}_3\text{-ZnO-CaO-Nb}_2\text{O}_5$  ceramics. *Ferroelectrics* 262(1): 65–70.
- Yanping, L., Xi, Y., Desheng, Z. and Liangying, Z. 2001b. Effect of NiO additive on structure and dielectric properties of  $\text{Bi}_2\text{O}_3\text{-ZnO-Nb}_2\text{O}_5$  based ceramics. *Ferroelectrics* 262(1): 59–64.
- Yin, Q., Zhu, B., and Zeng, H. 2009. Future development of functional ceramics. In *Microstructure, Property and Processing of Functional Ceramics*, ed. Q. Yin, B. Zhu and H. Zeng, pp 345–346. Beijing: Metallurgical Industry Press.

- Yonezawa, S., Muraoka, Y., Matsushita, Y. and Hiroi, Z. 2004. New pyrochlore oxide superconductor  $\text{RbOs}_2\text{O}_6$ . *Journal of the Physical Society of Japan* 73(4): 819–821.
- Zhang, S.S., Xu, K. and Jow, T.R. 2004. Electrochemical impedance study on the low temperature of Li-ion batteries. *Electrochimica Acta* 49(7): 1057-1061.
- Zheng, R.K., Wang, J., Tang, X.G., Wang, Y., Chan, H.L., Choy, C.L. and Li, X.G. 2005. Effects of Ca doping on the Curie temperature, structural, dielectric, and elastic properties of  $\text{Ba}_{0.4}\text{Sr}_{0.6-x}\text{Ca}_x\text{TiO}_3$  ( $0 \leq x \leq 0.3$ ) perovskites. *Journal of Applied Physics* 98(8): 084108.

